An Introduction to the Development and Use of the MASTER CURVE METHOD

Donald E. McCabe
John G. Merkle
Kim Wallin

ASTM INTERNATIONAL
Standards Worldwide

An Introduction to the Development and Use of the Master Curve Method

Donald E. McCabe, John G. Merkle, and Kim Wallin

ASTM Stock Number: MNL52

ASTM International
100 Barr Harbor Drive
PO Box C700
West Conshohocken, PA 19428-2959, USA

Printed in the U.S.A.

Library of Congress Cataloging-in-Publication Data

McCabe, Donald E., 1934–
An introduction to the development and use of the master curve method/ Donald E. McCabe, John G. Merkle, and Kim Wallin.
p. cm.—(ASTM manual series; MNL 52)
Includes bibliographical references and index.
ISBN 0-8031-3368-5 (alk. paper)
1. Structural analysis (Engineering) I. Merkle, J. G. II. Wallin, Kim.
III. Title. IV. Series.

TA645.M21 2005
620.1'126—dc22 2005007604

ISBN 0-8031-3368-5

ASTM Stock Number: MNL 52

Printed in Lancaster, PA
May 2005

Foreword

This publication, *An Introduction to the Development and Use of the Master Curve Method*, was sponsored by Committee E08 on Fatigue and Fracture and E10 on Nuclear Technology and Applications. It was authored by Donald E. McCabe, Consultant, Oak Ridge National Laboratory, Oak Ridge, Tennessee; John G. Merkle, Consultant, Oak Ridge National Laboratory, Oak Ridge, Tennessee; and Professor Kim Wallin, VTT Industrial Systems, Espoo, Finland. This publication is Manual 52 of ASTM's manual series.

Acknowledgments

The authors wish to acknowledge the Heavy-Section Steel Irradiation Program, which is sponsored by the Office of Nuclear Regulatory Research, US Nuclear Regulatory Commission, under interagency agreement DOE 1886-N695-3W with the US Department of Energy under contract DE-AC05-00OR22725 with UT Battelle, LLC, for supporting, in part, the preparation of this document. The authors also wish to express appreciation for the assistance provided by the ORNL-HSSI project manager, Dr. T. M. Rosseel, and for the manuscript preparation work of Ms. Pam Hadley and the graphics assistance of Mr. D. G. Cottrell.

Contents

1

Preface

THE PRESENT MANUAL IS WRITTEN AS EDUCATIONAL MATERIAL FOR non-specialists in the field of fracture mechanics. The intention is to introduce a concept that can be understood and used by engineers who have had limited exposure to elastic-plastic fracture mechanics and/or advanced statistical methods. Such subjects are covered in detail in USNRC NUREG/CR-5504 [1].

Section 2 explains why the application of fracture mechanics to ordinary structural steels has been delayed for so long. Underlying the explanation is a problem with a technical subject matter that has become, to a degree, unnecessarily esoteric in nature. The Master Curve method, on the other hand, addresses the practical design related problem of defining the ductile to brittle fracture transition temperature of structural steels directly in terms of fracture mechanics data. Section 2 describes the evolution of the method from a discovery phase to the development of a technology that can be put to practical engineering use (see Note 1).

> Note 1—Section 2 denotes stress intensity factors as K_{Ic} or K_{Jc}. The former implies linear elastic and the latter elastic-plastic stress intensity factor properties. K_{Ic} also implies that larger specimens had to be used.

Section 3 explains the data validity requirements imposed on test data and the number of data required to constitute a statistically useable data set for determining a reference temperature, T_o. The temperature, T_o, has a specific physical meaning with regard to the fracture mechanics properties of a material.

Section 4 describes the test specimens that can be used to develop valid K_{Jc} data. The recommended specimen designs optimize the conditions of constraint, while at the same time they require the least amount of test material to produce a valid K_{Jc} fracture toughness value. Care is taken to explain why certain other specimen types would be unsuitable for this type of work.

Section 5 presents, in simple terms, the fixturing and test equipment needs. Detailed descriptions are not necessary in the present manual, since *The Annual Book of ASTM Standards*, Volume 03.01, has several standard methods that present detailed information on fixtures that have been used successfully for the past 30 years. However, some of the lesser-known details relative to experience in the use of this equipment for transition temperature determination are presented herein.

Section 6 covers preparation of specimens for testing. The pre-cracking operation is an extremely important step, since, without sufficient care, it is possible to create false K_{Jc} data, influenced more by the pre-cracking operations than by accurately representing the material fracture toughness property.

Section 7 deals with test machines, their mode of operation, and recommended specimen loading rates. The usual practice of measuring slow stable crack growth during loading of test specimens is not a requirement when testing to

determine K_{Jc} values. This greatly simplifies the procedure. Post-test visual measurement of the crack growth that has occurred up to the point of K_{Jc} instability is required, however.

Section 8 presents all of the information needed to calculate values of K_{Jc}. Some K_{Jc} data may have to be declared invalid due to failing the material performance requirements discussed in Section 3. Contrary to the implication in other ASTM Standards that invalid data are of no use, this method makes use of such data to contribute to the solution for the T_o reference temperature. The only data to be discarded as unusable are data from tests that have not been conducted properly.

Section 9 contains the statistical equations that produce the fracture toughness, "scale parameter," for the material tested. The only complexity involved is the determination of substitute (dummy) K_{Jc} values, which must replace invalid K_{Jc} values to be substituted into the calculations. The "scale parameter" is calculated and used in expressions given in Section 10 to calculate the reference temperature, T_o, which indexes the Master Curve.

Section 10 includes a second option for calculating the T_o temperature that is useable when the K_{Jc} data have been generated at varied test temperatures. In this case, test temperature becomes an added variable in the calculation.

Section 11 shows how the variability of K_{Jc} values is handled using the three-parameter Weibull model. Tolerance bounds that will bracket the data scatter can be calculated with associated confidence percentages attached to the bounds. Also included is reality-check information that sets limits, or truncation points, outside of which the ductile to brittle-transition (Master Curve) characterization of a material may not be represented by the test data.

Section 12 presents information on work in progress. The pre-cracked Charpy specimen, if proven to be viable for the production of fracture mechanics data, would greatly expand the applications for the Master Curve procedure. This specimen, because of its small size, taxes the limit of specimen size requirements, so that a classification of work in progress is warranted at the present time. Another subject introduced is a proposal for dealing with macroscopic metallurgical inhomogeneity of the steel being tested. Some steel products, such as heavy-section steel plate, can have fracture toughness property variations that are a significant function of the through-thickness position. The Master Curve concept, unmodified, is not well suited for dealing with such macroscale inhomogeneity. In this particular case, the recommended approach that is suggested herein is only a subject for future evaluation.

Section 13 contains a brief discussion of important considerations involved in directly applying Master Curve fracture toughness data to the fracture-safety analysis of actual structures.

Appendices taken directly from standard E 1921-03 [19] have been added to the present document, since they contain example problem solutions for Sections 10.1, 10.2, 11.1, and 11.3 of the present manual. These problems can be used as self educational material to familiarize the user of the manual with the computational steps involved with the determination of the Master Curve reference temperature, T_o.

1.1—Nomenclature

A_p Area of plastic work done on test specimens; MJ, in.•lb

$A_{p(ff)}$ Plastic area determined from load-front face displacement test records; MJ, in.•lb

a or a_p	Physical crack size; meters, inches
B	Gross thickness of specimens; meters, inches
B_N	Net thickness of side-grooved specimens; meters, inches
B_x	Thickness variable, x, that represents the specimen thickness of prediction, meters, inches
B_1	The thickness of the specimens that were tested; meters, inches
B_4	Four-inch thick specimen; 0.1016 meters, 4-in., $B_x = 4$
B_e	Effective thickness of side grooved specimens used in normalized compliance, meters, inches
b	Weibull exponent; sometimes evaluated empirically, but in E 1921, used as a deterministic constant, 4, in all equations where fracture toughness is in units of K, and 2 for toughness in units of J
b_o	Initial remaining ligament length in specimens; meters, inches
C_n	Compliance, (V_{LL}/P) normalized by elastic modulus (E′) and effective thickness (B_e)
C	In Eq 21, a constant established by correlation between T_o and T_{CVN} transition temperature, °C
D_1	Coefficient in Eq 30 for establishing tolerance bounds, MPa$\sqrt{m}$
D_2	Coefficient in Eq 30 for establishing tolerance bounds, MPa$\sqrt{m}$
E'	Nominal elastic modulus established for ferritic steels; 206, 820 MPa, 30×10^6 psi
$f(\frac{a}{W})$	A dimensionless function that reflects the geometry and mode of loading of the specimen
H	Half height of a compact tension specimen, Fig. 7, meters, inches
i	Incremental order for test data, namely i increments from 1 to N
J	A path independent integral, J-integral; MJ/m^2, in.•lb/in.^{2}
J_e	Elastic component of J determined using K_e; MJ/m^2, in.•lb/in.^{2}
J_p	Plastic component of J determined using A_p; MJ/m^2, in.•lb/in.^{2}
J_c	J-integral measured at the point of onset of cleavage fracture, MJ/m^2, in.•lb/in.^{2}
J_{Ic}	J-integral measured at the point of 0.2 mm of slow-stable crack propagation, E 1820, MJ/m^2, in.•lb/in.^{2}
K_{Ic}	Plane strain stress intensity factor determined according to the requirements of E 399; MPa$\sqrt{m}$, ksi$\sqrt{in}$.
K_{Ia}	Stress intensity factor at crack arrest determined according to the requirements of E 1221; MPa$\sqrt{m}$, ksi$\sqrt{in}$.
K_{Jc}	Stress intensity factor determined by conversion from J_c;. MPa$\sqrt{m}$, ksi $\sqrt{in}$.
K_J	Final values of K (from J) where there was no cleavage instability involved; MPa$\sqrt{m}$, ksi$\sqrt{in}$.
$K_{Jc(limit)}$	The maximum value of K_{Jc} data where K_{Jc} can be considered valid, MPa$\sqrt{m}$, ksi$\sqrt{in}$.
K_{CENS}	A special type of K_{Jc} censored value used in the SINTAP data treatment procedure Section 12.2.1, MPa$\sqrt{m}$, ksi$\sqrt{in}$.
$K_{Jc(x)}$	The predicted K_{Jc} value for a specimen of size B_x, MPa$\sqrt{m}$, ksi$\sqrt{in}$.
$K_{Jc(med)}$	The median of a K_{Jc} data distribution for which $P_f = 0.5$, MPa$\sqrt{m}$, ksi$\sqrt{in}$.
K_o	A K_{Jc} value that represents the 63 percentile level of a K_{Jc} data distribution, MPa$\sqrt{m}$, ksi$\sqrt{in}$.

$K_o(T)$	K_o for a data distribution determined at test temperature, T, MPa$\sqrt{m}$, ksi$\sqrt{in}$.
K_{min}	A deterministic constant of the Weibull distribution, 20 MPa$\sqrt{m}$, 18 ksi$\sqrt{in}$, Eq 7
K_{max}	The peak K_e of the fatigue pre-cracking cycle, MPa$\sqrt{m}$, ksi$\sqrt{in}$.
K_e	A linear-elastic stress intensity factor, MPa$\sqrt{m}$, ksi$\sqrt{in}$.
R	In fatigue pre-cracking, the ratio $R = K_{min}/K_{max}$
N	Number of data, sum of valid plus invalid data
P_f	Probability of failure for a specimen, chosen at random from an infinite population of specimens, to fail at or before the K_{Jc} of interest
r	The number of valid K_{Jc} data, exclusive of all invalid data
P	Load; MN, pounds
T	Test temperature; °C
T_i	Test temperature of the i^{th} specimen in the incremental order, see Eq 26; °C
T_o	The Master Curve reference temperature, see Eqs 10 and 11; °C
T_Q	For testing with unrecommended specimens, a test temperature at which median K_{Jc} equals 100 MPa$\sqrt{m}$. T_Q is not used to establish the Master Curve
V_{LL}	Specimen displacement measured on the plane of loading; meters, inches
V_{ff}	Specimen displacement measured at the front face location, see Fig. 7; meters, inches
W	Specimen width denoted in Figs. 7 and 8, meters, inches
$Z_{(xx)}$	Standard normal deviate at cumulative probability level, P_f = xx

Greek Symbols

Δa_p	Slow-stable crack growth prior to the onset of cleavage fracture, mm, inches
ΔT_o	The increment to T_o that corresponds to one standard deviation; °C
σ_{To}	One standard deviation expected on multiple T_o determinations; °C
σ_{ys}	Material yield strength (temperature sensitive); MPa, ksi
θ	Scale parameter; units of J in Eq 3, units of $(K_o - K_{min})$ in Eq 27, MJ/m^2, in.•lb/in.^{2}
η_p	Plastic eta; a dimensionless coefficient that converts plastic work done on specimens into the plastic component of the J-integral
$\eta_{p(cmod)}$	Plastic eta modified to account for measuring displacement at the crack mouth position of SE(B) specimens, see Fig. 8
Γ	Gamma function, obtainable from handbooks of mathematical functions
δ_i	Kronecker delta; either one or zero: (1) used for valid K_{Jc} entries, and (0) for dummy value entries in Eq 26.

Specimen Size (nT) (see Figs. 7 and 8)

½ T,B = ½ in.
1T,B = 1 in.
4T,B = 4 in.

2 Background

2.1—Historical Aspect

FRACTURE MECHANICS IS A RELATIVELY NEW SCIENTIFIC DISCIPLINE that has effectively added a useful advancement to the technology of the mechanics of materials. Fracture mechanics provides the tools to compute the capability of brittle materials to sustain cracks stably while under load (stress). This new technology has been most successfully applied to aerospace materials, which usually have ultra-high strength and, therefore, are usually highly frangible. More recent attempts to adapt this new technology to structural steels has encountered added difficulties, and considerably more technological development had to be undertaken. Specifically, the added difficulty results from the combination of higher fracture toughness and lower yield strength, resulting in more plastic deformation involved in the fracture toughness development process. Consequently, several elastic-plastic analysis procedures have been introduced [1–3], of which the most widely used has been the J-integral approach, conceived in the early 1970s. However, until recently, the main use of J has been for the characterization of ductile tearing resistance in terms of J-R curves and J_{Ic} [4,5].

Structural steels also differ from aerospace materials in another way. Ferritic structural steels suffer significant fracture toughness loss with decreasing temperature, displaying a transition temperature at which the fracture mode changes from fully ductile to increasing amounts of brittle cleavage fracture. J-R curve studies dealing with the characterization of ductile tearing have been useful only for that particular mode of fracture. On the other hand, the property of most importance in structural steel applications is the identification of the ductile-to-brittle transition temperature. The application of elastic-plastic fracture mechanics to this problem has been slow, because technically difficult obstacles were encountered. The K_{Ic} specimen size requirements of ASTM Standard E 399 were designed to provide lower bound fracture toughness estimates for aerospace materials [6]. These same requirements, applied to structural steels, lead to impractically huge specimens that are not amenable to routine laboratory testing. Additionally, instead of finding a consistent lower bound of fracture toughness, extreme data scatter develops in the ductile-to-brittle transition range.

An ad hoc PVRC task group was formed in the early 1970s [7] to develop a fracture mechanics methodology for pressure vessel steels to be included in Section III of the ASME Code. Lacking any precedent, the task group collected all available valid dynamic initiation, K_{Ic}, and crack arrest, K_{Ia}, fracture toughness transition temperature data, as well as the accompanying Charpy impact and drop-weight data. To put all the data on the same transition temperature footing, the various test temperatures were normalized to a transition temperature, termed RT_{NDT}, which had its origin in an older test method that was not directly fracture-mechanics related [8]. Out of necessity, and to achieve continuity with existing data, a relationship between the empirical test method and fracture mechanics tests was

postulated. About 100 K_{Ic} toughness values were plotted against normalized test temperature, (T-RT_{NDT}), and the height of the data scatter band, in terms of toughness, encompassed about a factor of three between the lowest to the highest values. For conservatism, the approach selected was to draw an underlying curve, postulating at the same time that this curve would be a universal lower bound curve for all ferritic pressure vessel steels. This approach of defining a lower bound fracture toughness curve has remained in place for almost 30 years [9,10]. It has recently been modified to use the static data only for crack initiation [11].

New ideas about cleavage fracture began to emerge starting in about 1980 [12], and there has been continuous progress made ever since, culminating only recently in the Master Curve concept and ASTM Standard E 1921-97, "Determination of Reference Temperature, T_o, for Ferritic Steels in the Transition Range." Modern statistical methods, and an improved understanding of elastic-plastic test methods, have been coupled to define a transition curve of static fracture toughness versus temperature that is derived using only fracture mechanics-based test data. The uncertainty associated with the empirical postulates involving non-fracture mechanics data that had to be employed in the 1970s has been eliminated. The reason for significant data scatter, even under controlled constraint conditions, can now be explained. Specimen size effect on material fracture toughness at a given temperature is better understood. Consequently, the definition of a transition temperature for a given material can be improved by directly applying fracture mechanics test data and statistical analysis to determine the characterizing temperature, T_o. The key elements of the new methodology are as follows:

1. Data scatter is recognized as being due to randomly sized and distributed cleavage-crack triggering sources contained within the typical microstructure of ferritic steel. A three-parameter Weibull cumulative probability statistical model is used to suitably fit observed data scatter. Elastic-plastic fracture toughness values are expressed in units of an equivalent elastic stress intensity factor, K_{Jc}.
2. J-integral at the point of onset of cleavage instability, J_c, is calculated first and converted into its stress intensity factor equivalent as K_{Jc}. It has been demonstrated that specimens can be $1/40^{th}$ of the size required for K_{Ic} validity by ASTM Standard E 399 and still maintain sufficient control of constraint.
3. The specimen size effect observed in transition range testing is quite subtle, and the most accurate modeling of this effect uses a weakest link assumption, derived from the observations discussed above in Item 1. The application of this model enables conversion of K_{Jc} data obtained from specimens of one size to values for specimens of another size.
4. Use of the above three items has made it possible to observe that most ferritic steels tend to conform to one universal curve of median fracture toughness versus temperature for one-inch thick specimens [13]. Hence, the existence of a universal "Master Curve" has been demonstrated. Although the Master Curve corresponds to one fixed specimen size, size effect is sufficiently subtle, so that the general approach appears to be directly applicable in a number of engineering situations.

2.2—Concept Discovery (Landes/Shaffer [12])

The data scatter problem referred to in Section 2.1 has been observed from time to time during the past half century of transition range testing [14]. However, the

experimental and data-analysis practices used during most of this period were, for the most part, simply based, which invited the explanation for data scatter to be dismissed as test-method related. In later years when the more refined facture mechanics test practices were applied to structural steels, such as nuclear pressure vessel plate, data scatter due to test material microstructure became more evident. Attention to the data scatter situation did not happen until about 1980, when Landes and Shaffer considered the application of a statistical rationale [12]. They were able to demonstrate that the data scatter observed from multiple tests made on a NiMoV generator-rotor steel could be described, as illustrated by Fig. 1, with the following two-parameter Weibull statistical model:

$$P_f = 1 - \exp - \left(\frac{J_c}{\theta} \right)^b \tag{1}$$

where P_f is a cumulative probability of fracture at J_c for an arbitrarily selected specimen loaded to that particular J-integral level; θ is a scale parameter, viz the J level at the 63.2 % failure probability level, and b is the empirical Weibull slope of the model.

Equation 1 defines the J_c cumulative failure probability distribution for a finite sample drawn from an infinite population of data for the test material. The available data were ranked in ascending order according to J_c fracture toughness at instability and assigned a cumulative probability value according to the following rank estimator equation:

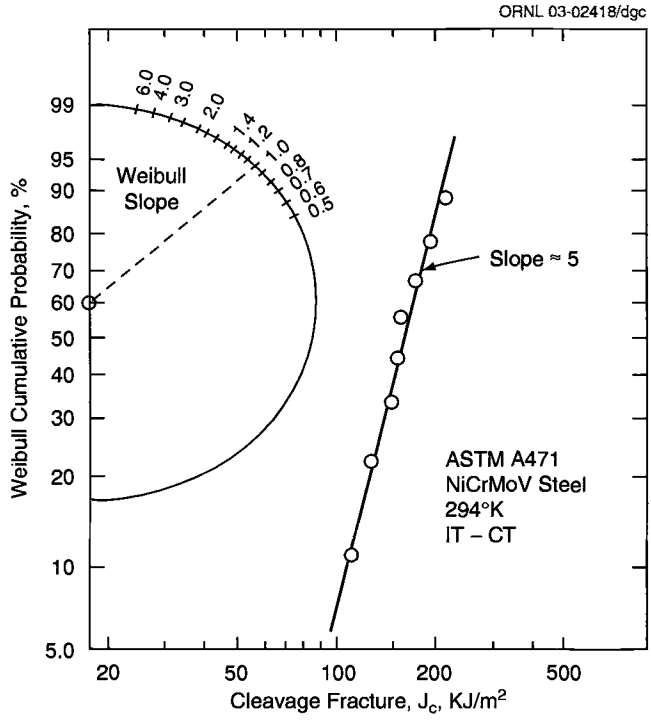

Fig. 1—Failure probability versus J_c plotted in Weibull coordinates (from Landes and Shaffer [12]).

$$P_f = i/(N+1) \tag{2}$$

where i is the rank order number, from 1 to N, and N is the number of J_c data available.

When the N data values are plotted on a graph with Weibull coordinates, a fitted straight line defines the two Weibull parameters, θ and b, in Eq 1. See Fig. 1.

This work in Ref. [12] was followed up by a careful examination of the fracture surfaces. The authors noted that there were apparent trigger points on the fracture surfaces at which the cleavage cracks had initiated, and more importantly, there appeared to be some correlation between the trigger point separation distance from the initial crack front and the J_c values at instability for the specimens. Hence, Landes and Shaffer concluded that the J_c data scatter was a weak-link phenomenon amenable to statistical analysis. This observation was later reinforced in a paper by Heerens and Read [15].

Landes and Shaffer [12] then surmised that Eq 1 could be used to predict a specimen size effect on J_c fracture toughness due to this weakest link postulate. Equation 1 was rearranged to express the probability of survival ($1-P_f$) for specimens of various sizes. Test data for size, e.g., 1T (1-in. thickness), is thus expressed:

$$\left[1 - P_{f(1T)}\right] = \exp - \left(\frac{J}{\theta}\right)^b \tag{3}$$

If a 4T specimen were tested, the highly stressed volume of material loaded to the same J_c value must have the lesser joint probability, $[1-P_{f(1T)}]^4$, of survival. Hence, for the 4T size:

$$[1 - P_{f(4T)}] = [1 - P_{f(1T)}]^4 = \exp - 4\left(\frac{J_c}{\theta_{1T}}\right)^b \tag{4}$$

For equal values of P_f to be given by Eqs 3 and 4, the size effect is given by:

$$J_{c(4T)} = J_{c(1T)} \left(\frac{B_1}{B_4}\right)^{1/b} \tag{5}$$

where B_1 = 25.4 mm (1-in.), and B_4 = 101.6 mm (4-in.).

Equation 5 can be generalized by substituting a generic size x for size 4.

2.3—Engineering Adaptation (Wallin [17])

The early observations of Landes and Shaffer [12], and Landes and McCabe [16] provided the keystone ideas that led to the extensive work of Wallin in the development of a more useful engineering version of the concept [17]. Specifically, fracture toughness expressed in units of elastic-plastic stress intensity factor, K_{Jc}, is amenable to direct calculation of a critical flaw size or the critical stress (load), given an assumed existing flaw. The relationship between J_c and K_{Jc} is simply:

$$K_{Jc} = (E'J_c)^{1/2} \tag{6}$$

The above terms are defined in the Nomenclature.

Absent from the early work was the observation that steels usually exhibit an absolute lower shelf of fracture toughness at temperatures below the transition range. Equation 1 suggests that there is a finite probability that J_c can approach

zero fracture toughness, given sufficient numbers of replicated data. Wallin [17] assembled a K_{Ic} data set to perform a sensitivity study using the following three-parameter Weibull model:

$$P_f = 1 - \exp\{-[(K_{Jc} - K_{min})/(K_o - K_{min})]^b\} \quad (7)$$

The above terms are defined in the Nomenclature.

The scale parameter in this case is $(K_o - K_{min})$. Monte Carlo sampling of the data population was repeatedly performed with varied sample sizes, N. This work led to the very important observation that when K_{min} of Eq 7 is set equal to 20 MPa $\sqrt{m}$, the Weibull slope, b, for a complete data population, approaches 4, but it can only be evaluated accurately when sample size, N, is sufficiently large (e.g., of the order of 100 specimens). See Fig. 2. The 95 % confidence bounds on the mean Weibull slope for the Monte Carlo simulations are shown in Fig. 2 along with the confirming data sources that the author was able to locate in 1984. The importance of this work is the determination that two of the three parameters in Eq 7, K_{min} and b, both of which would require huge numbers of specimens to find by experiment, can be treated as known constants. As will be explained presently, the third parameter $(K_o - K_{min})$, MPa $\sqrt{m}$, requires only reasonable numbers of replicate data.

The validation of Eq 7 using experimental data has been an ongoing activity since 1984. More recently developed data for which there were at least 20 data replications are presented in Table 1. The best fit Weibull slopes for these data were determined by linear regression. Experience has shown that best fit Weibull slopes and K_{min} determinations from small data sets cannot be expected to accurately predict the true Weibull slopes of total data populations.

TABLE 1—Weibull slopes and values of T_o determined by linear regression for data sets with 20 or more duplicate specimens (K_{min} set at 20 MPa $\sqrt{m}$).

Material Source	Material	Test Temperature (°C)	Specimen Size (T)	Number of Specimens	Best Fit Slope	T_o by Maximum Likelihood (°C)
MPC-JSPS round robin	A 508 Class 3	−50	1	47	3.75	−105
		−75	1	55	5.80	−105
		−100	1	50	4.30	−109
Ando, 1992	SM41C	−70	1.2	20	3.40	−126
Faucher	Algoma LT 60	−120	0.4	23	3.30	−126
ORNL	A553 grade B, HSSI Plate13A	−75	1	25	3.00	−77
		−75	1/2	20	5.20	−79
Iwadate, 1991	A 508 Class 3	−60	1/2	30	4.55	−44
		−20	1/2	28	3.44	−41
	A 470	−100	1/2	27	4.58	−90
		−60		26	3.82	−74

TABLE 2—MPC/JSPS round robin data for tests made at -100°C (best fit slopes by regression).

Lab	Weibull Slope	Number of Specimens	Median* K_{Jc} MPa $\sqrt{m}$)	T_o °C
A	5.0	5	109.7	–107
C	3.0	5	117.9	–112
E	4.0	5	122.0	–114
F	5.4	5	111.6	–108
G	5.6	5	101.2	–101
H	5.1	5	106.0	–104
L	11.3	5	131.9	–123
M	3.4	5	93.9	–95
Q	3.9	5	128.3	–119
R	2.8	5	105.9	–104
Grand Total	4.3	50	113.6	–109

*1σ = 12.1 MPa $\sqrt{m}$; ($K_{Jc\,(med)} \pm 2\sigma$) = 89.4 to 137.8.

Following up on the weakest-link specimen size effect model of Eq 5, the same rationale applied to Eq 7 leads to the following:

$$K_{Jc\,(x)} = K_{\min} + \left(K_{Jc\,(1)} - K_{\min}\right)\left(\frac{B_1}{B_x}\right)^{1/b} \tag{8}$$

The terms that appear in the above expression are defined in the Nomenclature.

Hence, the weakest-link-based model of Eq 8 allows the data from any given specimen size to be converted to that for a common reference specimen size of choice. For Master Curve development, to be discussed in Section 2.5, the common specimen size used is 25.4-mm (1-in.) thickness.

2.4—Application to Round Robin Data

An interlaboratory round robin activity that involved 18 laboratories located in the United States, England, and Japan was jointly sponsored by the Materials Property Council (MPC) and the Japan Society for the Promotion of Science (JSPS) [18]. About 150 K_{Jc} data were developed from a single plate of A508, Class 3 pressure vessel steel. Each participating laboratory had the option to choose one, two, or all three of the assigned test temperatures of –50°, –75°, and –100°C. Five 1T size compact specimens were provided for each selected test temperature. The apportionment scheme resulted in almost equal numbers of specimens being tested at each test temperature: about 50 specimens at each. This round robin was started in 1989, which was about eight years prior to the issuance of ASTM Standard E 1921-97 [19]. Hence, it is likely that the test practices used by the participating laboratories were not necessarily uniform. Despite this fact, the data did not give any evidence of problems due to test practice variations.

Table 2 is used herein to illustrate the outcome. Each data set of five specimens was evaluated for the implied Weibull slope, and then all the data were combined for the 50-specimen population. All but one laboratory, L, had slopes within the 95 % confidence bounds (for N = 5) of Fig. 2. Most of the predicted median K_{Jc}

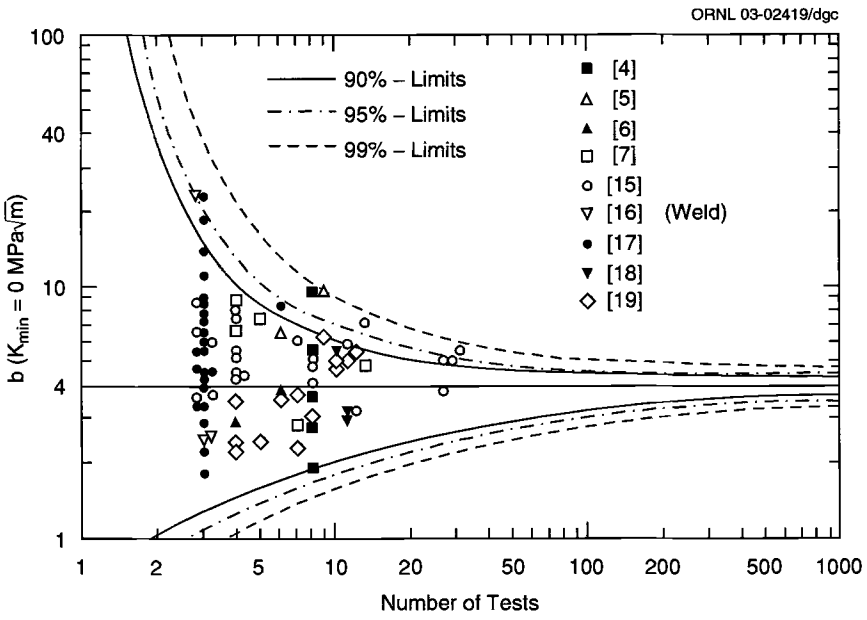

Fig. 2—Theoretical confidence bounds on Weibull slopes established using a Monte Carlo method and experimental Weibull slopes, b, determined on data from nine references, the identifying numbers for which are as listed in [17].

values were reasonably close to the combined median of 113.6 MPa $\sqrt{m}$. Figure 3 shows the round robin data for all three test temperatures plotted in Weibull coordinates. The straight lines shown came from Eq 7 rearranged. The Weibull slope was set equal to 4, and K_{min} was set equal to 20 MPa $\sqrt{m}$. The method of obtaining the scale parameter ($K_o - K_{min}$) will be covered in Section 9. The good fit to the experimental data at the three test temperatures suggests that the model of Eq 7, with two deterministic parameters (K_{min} and the Weibull slope b), tends to be independent of test temperature.

2.5—Master Curve

ASTM Standard Method E 1921-97 [19] presents the experimental and computational procedures that are to be used to arrive at a reference temperature, T_o. Temperature T_o is defined as the temperature at which a set of data having six or more valid K_{Jc} values (as defined by the method), obtained with 25.4-mm (1-in.) thick specimens, will have a median K_{Jc} of 100 MPa $\sqrt{m}$. Alternatively, specimens of another size, with K_{Jc} values converted to 25.4-mm (1-in.) size equivalence using Eq 8, will also develop a median K_{Jc} of 100 MPa $\sqrt{m}$. The Master Curve is an empirically derived universal transition range curve of fixed shape for static fracture toughness versus temperature. It is known to characterize the transition range of commercially made ferritic steels when the data are developed using fracture mechanics methods. Temperature T_o is the reference temperature that positions the Master Curve on a plot of K_{Jc} versus test temperature. Justification for the

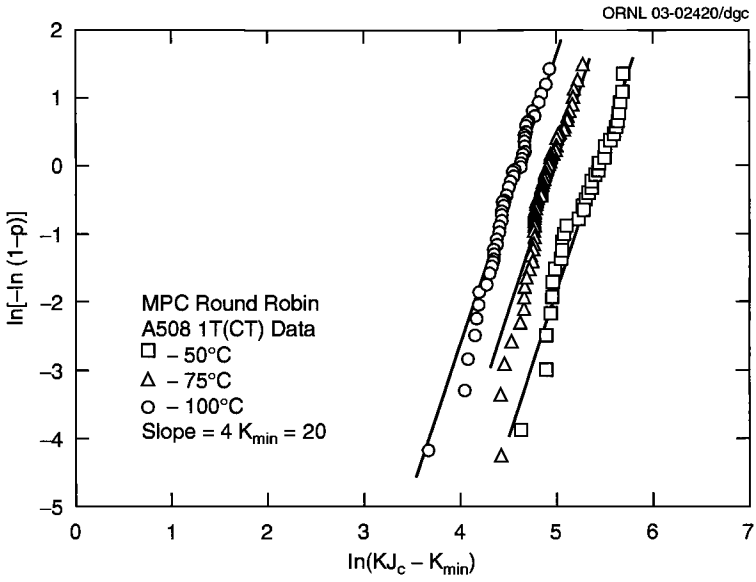

Fig. 3—Data taken from the MPC/JSPS round robin activity, plotted in Weibull coordinates showing constant Weibull slopes independent of test temperature.

premise stated above is based on a substantial amount of supporting experimental evidence [1].

Although the above universal curve assertion may seem to be a surprising suggestion at first, this is not the case. As had been pointed out before, the ASME Code [9,10] has used such a postulate for almost 30 years in the form of the so-called lower bound K_{Ic} and K_{Ia} curves. These curves have been used to set fracture toughness requirements for crack initiation and crack arrest conditions in nuclear reactor pressure vessel steels. The Master Curve work essentially verifies the ASME postulate, differing principally in the reference temperature indexing method, using T_o instead of RT_{NDT} and a median transition curve shape instead of K_{Ic} lower bound.

2.5.1—Median Versus Scale Parameter Option

The choice of the failure probability level, P_f (given by Eq 7), for Master Curve definition was optional. Curves for two probability levels can be found in the literature [13,19]. One is for $P_f = 0.632$, chosen to represent the probability level corresponding to the scale parameter, $(K_o - K_{min})$. At this probability, $(K_{Jc} - K_{min}) = (K_o - K_{min})$, and the power term in Eq 7 is negative unity. This level of K_{Jc} is convenient when making statistical calculations. The other convenient value of P_f is 0.5, the median of the distribution. The relationship between the parameter, K_o, and the K_{Jc} median is:

$$K_{Jc\,(med)} = [ln(2)]^{1/4}(K_o - 20) + 20, \quad \text{MPa}\sqrt{m} \tag{9}$$

The master curve representations (for 1-in. thick specimens only) are as follows:

for $P_f = 0.50$:

$$K_{Jc(med)} = 30 + 70\exp[0.019(T - T_o)], \quad \text{MPa}\sqrt{m} \tag{10}$$

for $P_f = 0.63$:

$$K_o = 31 + 77\exp[0.019(T - T_o)], \quad \text{MPa}\sqrt{m} \tag{11}$$

Hence, at a test temperature equal to T_o, $K_{Jc(med)}$ for a 1T specimen is 100 MPa $\sqrt{m}$, and K_o is 108 MPa $\sqrt{m}$. The equation for K_{Jc} median, Eq 10, was chosen for use in Standard E 1921, because of the definition of T_o and because it visually demonstrates the equality of data scatter above and below the Master Curve. See Fig. 4. Additionally, both coefficients of toughness are integers. Otherwise the difference between choosing between using Eqs 10 and 11 to determine T_o temperature is minor. There is only a very small difference in calculated T_o values, since the constants in Eq 11 are rounded off from 30.96 and 76.72.

2.5.2—Supporting Evidence

Obtaining experimental evidence in support of Eq 10 or Eq 11 has been the subject of ongoing research reported in the literature and technical reports for over 19

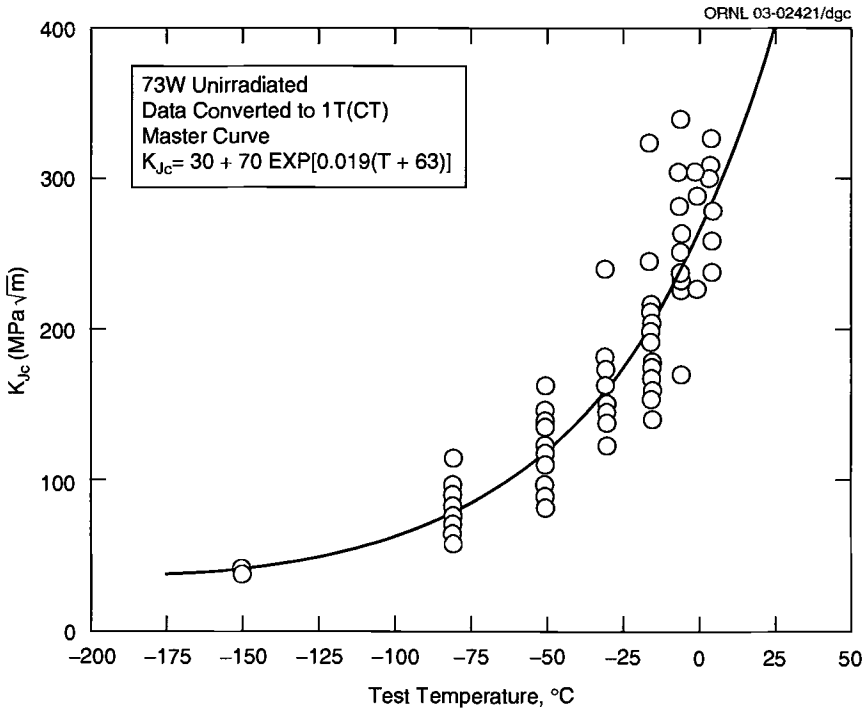

Fig. 4—K_{Jc} data scatter about the Master Curve, for weld-metal 73 W of the HSSI Fifth Irradiation series; specimen size varied from 1T(CT) to 8T(CT), and all data shown were converted to 1T(CT) equivalence. $T_o = -63°$.

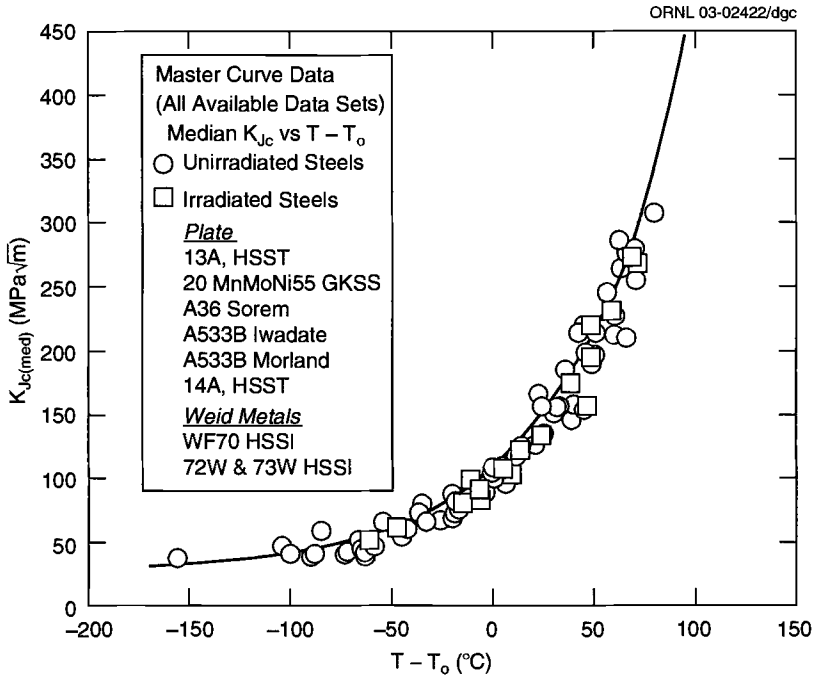

Fig. 5—Median K_{Jc} values from eight data sources; all data have been converted to IT equivalence, and test temperature normalized to T_o temperature.

years. The supporting technical document for E 1921 mentioned in Section 1.0 [1] contains 26 individual examples of fitting the Master Curve to transition range K_{Jc} data. Materials evaluated include base metals, weld metals, and in many cases, nuclear-related pressure vessel steels in the as-received and irradiated conditions. Figure 5 is a collection of such data with the materials identified only as base metal versus weld metal. The material identifications appear in the plot.

3

K_{Jc} Data Validity Requirements

ASTM STANDARD E 1921 REQUIRES THAT SPECIMENS BE MACHINED to certain proportionality and precision requirements. Most important for obtaining good data is that the specimens should be fatigue pre-cracked exactly as specified. Test machines must have calibrated load cells, and test fixturing should be aligned properly.

In all cases, at least six valid K_{Jc} data are required to determine a valid value of T_o. Standard E 1921 differs from most other ASTM standards from the standpoint that invalid data which fail provisional validity criteria are not completely rejected from the analysis procedure. Invalid data still provide information of relevance to the statistical model.

3.1—Data Duplication Needs

Accurate statistical modeling of a data population would normally require huge sample sizes. In the present case, the establishment of a fixed lower limit value, K_{min}, and a fixed shape of the distribution, defined by the Weibull slope, b, reduce the number of unknown parameters from three to one. The single parameter to be determined from the data sampling is the scale parameter, $(K_o - K_{min})$, which requires far fewer data to produce a reasonable estimate than if all three parameters had to be determined. Table 3 shows the results of an evaluation exercise used to arrive at the required sample size adopted in Standard E 1921. A Monte Carlo simulation was employed, using a data population of 50 K_{Jc} values obtained from the MPC/JSPS round robin activity previously cited in Section 2.4. Sample sizes ranged from 3 to 20, with sample size and the calculations for each sample size repeated 100 times. The standard deviations on the $K_{Jc\,(med)}$ determinations appear in the right column. The choice of a minimum sample size had to be based on a compromise between a slowly decreasing standard deviation and a practical number of specimens for an ASTM standard. The minimum practical sample size range is between 5 and 8 replicate specimens. Since there was very little gain in precision within this range, the sample size of 6 was selected. For critical evaluations, a conservative offset to T_o can be obtained by using a margin adjustment, to be discussed in Section 11.3.

3.2—Specimen Size Requirements

Specimen types and remaining ligament dimensions, to be discussed in Section 4, are set to maximize both constraint and K_{Jc} validity capacity. Only a certain amount of plastic deformation can be tolerated before excessive loss of constraint alters the K_{Jc} data distribution. The condition at the onset of this phenomenon has been estimated by theory and is also supported by experimental data [1,20]. The resulting criterion is given by the rules regarding specimen size and constraint.

TABLE 3—Average $K_{JC(med)}$ and standard deviation values for 100 Monte Carlo simulations, MPC/JSPS data at –100°C.

Sample Size N	Average $K_{Jc\ (med)}$ MPa $\sqrt{m}$	Standard Deviation MPa $\sqrt{m}$
3	113.7	13.1
4	111.8	11.5
5	113.2	9.3
6	112.9	9.2
7	113.0	8.2
8	113.2	7.9
9	112.6	7.6
10	113.2	7.0
15	113.4	5.8
20	113.3	5.0
50*	113.6	...

*population.

$$K_{Jc(\text{limit})} = (E'\sigma_{ys}b_o/30)^{1/2} \tag{12}$$

All terms in the above are defined in the Nomenclature. Other validity criteria are:

1. Test specimens that fail by cleavage when $K_{Jc} > K_{Jc\ (limit)}$ are invalid.
2. Test specimens that do not fail and remain ductile to the end of test, and for which $K_J > K_{Jc\ (limit)}$ are invalid.
3. A test for which loading is terminated without failure by cleavage before $K_{Jc\ (limit)}$ is reached is a non-test, and the datum is to be discarded.

3.3—Limit on Slow-Stable Crack Growth, Δa_p

If the slow-stable crack growth prior to the onset of K_{Jc} instability exceeds 1 mm (0.04 in.), the K_{Jc} value is to be classified as invalid. It is not necessary to use autographic equipment or digital analysis methods to follow the stable, ductile, crack advance during the test. Instead, post-test visual measurement of crack growth on the fracture surface can be used. Be sure to melt and remove, by drying, any frost layer from the fracture surfaces immediately after the test is completed to prevent obscuring the fracture surface due to oxidation. If crack growth measurement is to be delayed (for days), then protect the surfaces with a light oil. The method of measuring the depths of the initial fatigue pre-crack, and stable growth, is illustrated in Fig. 6 [21]. Crack depths are measured at nine symmetrically and equally-spaced, through-thickness locations. The two outside measurements are averaged, and this value is averaged with the remaining seven measurements to determine crack depth. Crack depth is referenced from the load line for compact specimens and from the front face for bend bar specimens.

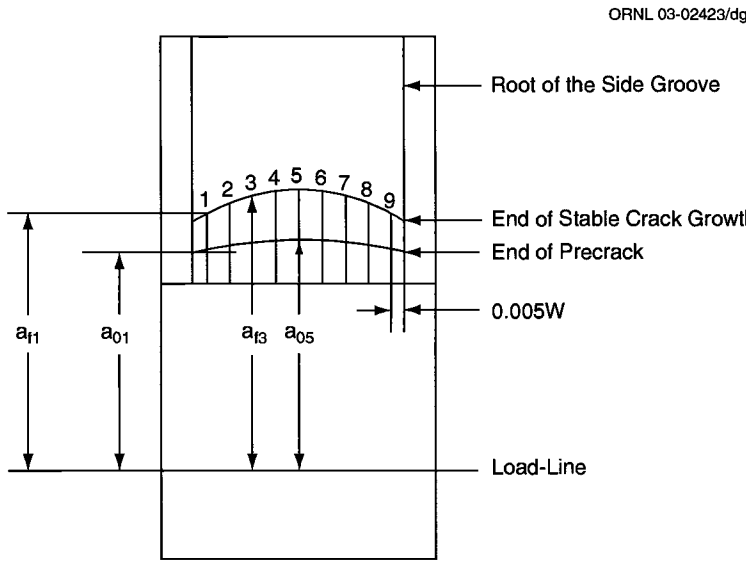

Precrack Length, $a_0 = 0.125\ [0.5(a_{01} + a_{09}) + a_{02} + \ldots a_{08}]$

Final Crack Length, $a_f = 0.125\ [0.5(a_{f1} + a_{f9}) + a_{f2} + \ldots a_{f8}]$

Fig. 6—Illustration of the nine-point method to determine initial crack size, a_0, and post-test final crack size, a_f. Illustration from [21].

4

Test Specimens

THE SPECIMENS USED TO DETERMINE TRANSITION RANGE DATA ARE shown in Figs. 7 and 8. Three compact specimen designs are shown in Fig. 7, all of which have fixed height to width ratios, 2H/W of 1.2. Thickness B = W/2. The one specimen on the left has a machined-in slot that is too narrow for inserting a displacement-measuring clip-gage at the load line. J-integral calculations require the measurement of work done on the specimen (area under the load versus load point displacement test record), so that load-line displacement measurement is necessary. However, the displacement gage can be placed on the front face of the specimen at a position 0.25W in front of the load-line. Front face displacement, V_{ff}, is nominally a factor of 1.37 times the load-line displacement, V_{LL} [22], hence the area under a load versus V_{ff} plot will be 1.37 times the area under a load versus V_{LL} plot, enabling J-integral calculations to be based on either type of test record. An alternative would be to use the caliper-type "over-the-top gage" shown in Fig. 9. Use of this gage should be limited to materials of low fracture toughness, since specimens that fracture with high stored elastic strain energy may damage such gages. The other two compact specimen designs shown in Fig. 7 provide recesses for clip gages that are placed on the load-line. Both have small vertical faces onto which razor blade knife-edges can be spot welded. Razor blade steel is easily trimmed to the size and shape needed with ordinary sheet-metal shears.

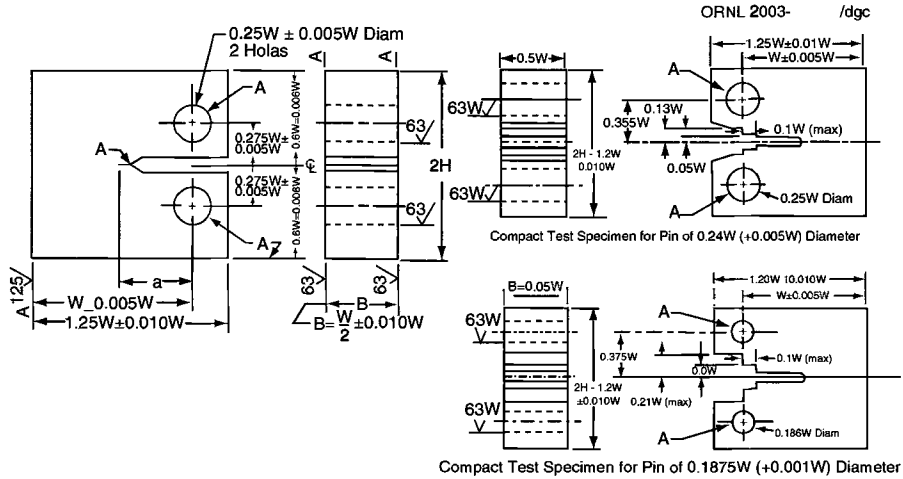

Note 1 – All surfaces shall be perpendicular and parallel as applicable to within 0.002W TIR.

Note 2 – The intersection of the crack start notch tips with the two specimen surfaces shall be equally distant from the top and bottom edges of the specimen within 0.006W TIP.

Fig. 7—Three optional compact [C(T)] specimen designs.

ORNL 2003- /dgc

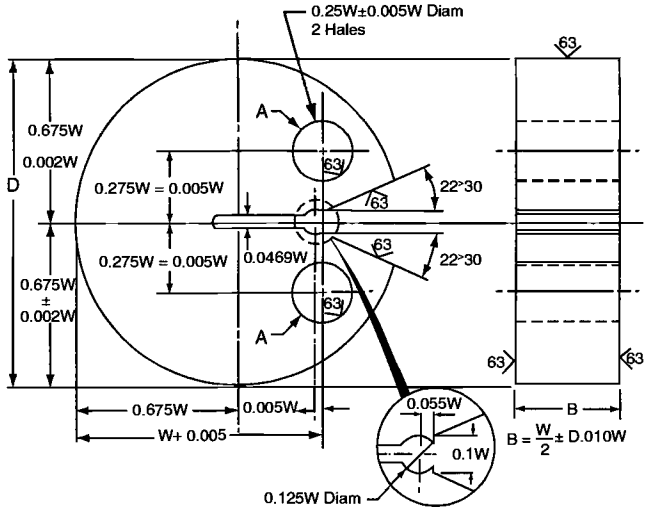

Note 1 – "A" surfaces shall be perpendicular and parallel as applicable to within 0.002W TIH.
Note 2 – The Intersection of the crack starter notch tips with the two specimen surfaces shall be equally distant from the top and bottom extremes of the disk within 0.005W TIR.
Note 3 – Integral or attached knife edges for dip gage attachment may be used.

Disk-shaped Compact Specimen DC(T) Standard Proportions

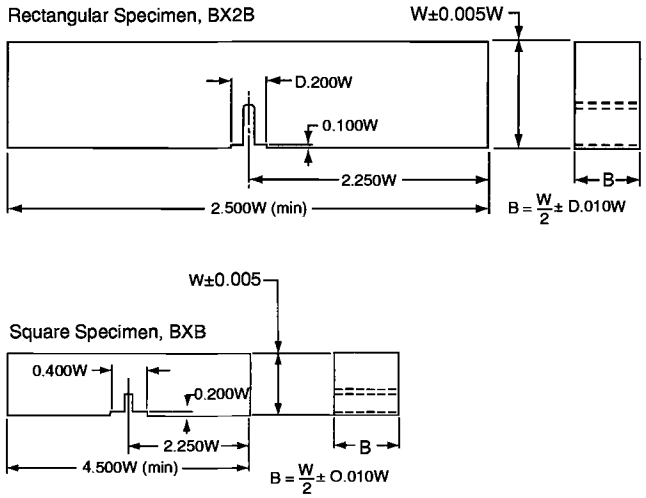

Note 1– All surfaces shall be perpendicular and parallel to within 0.001W TIR, surface finish 64v.
Note 2– Crack start notch shell be perpendicular to specimen surfaces to within +2°.

Recommended Bend Bar Specimen Design

Fig. 8—Alternate specimen, DC(T) and SEN(B), designs that can be used.

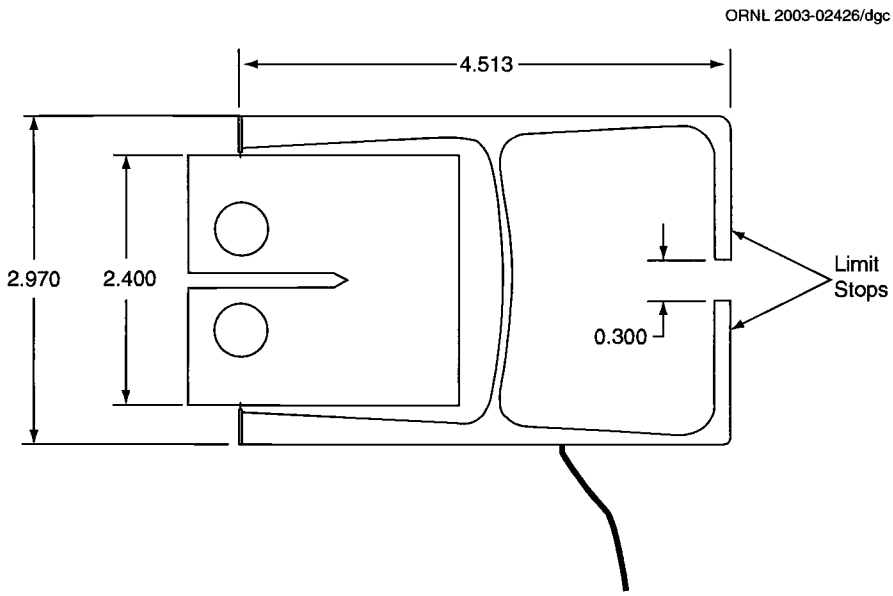

Fig. 9—An "over-the-top" clip gage, in this case for use on IT(CT) compact specimens. The design is that of J. Shepic. Dimensions are given in inches.

Figure 8 shows three specimens, the first of which is the disk-shaped compact specimen. This specimen has characteristics that are nearly the same as the standard compact specimens shown in Fig. 7. In the case of the disk-shaped compact specimen, the geometry is not conducive to a cut-out configuration, so it is necessary to machine integral semi-circular recesses in the profile at the load line, providing knife edges for clip gage attachment. Figure 8 also shows the two bend bar specimen designs. The standard bend bar specimens have a width to thickness ratio, W/B, of 2. The smaller bend bar has a W/B ratio equal to 1. The latter design is not the preferred geometry, but was adopted in E 1921 principally for use with specimens of pre-cracked Charpy design. Note that both bend bars have shallow under-cut surfaces machined on either side of the notch for measuring crack-mouth opening-displacement. Razor blades can be spot welded onto these surfaces with their beveled tips aligned with the specimen bottom face and a separation distance between the tips, allowing space for the insertion of a clip gage. The bend bar specimen is presently under study since it is not certain that T_o values derived therefrom are equal to T_o values obtained with compact specimens.

J-integral calculations are based on elastic plus plastic work absorbed by the specimens, so that the preferred test record is load versus load point displacement. Bend bars are three-point loaded using a total span of 4W, invariant of overall specimen size. Load point displacement is measured from the motion of the central transverse loading pin.

All of the specimen designs suggested in E 1921 are intended to create high constraint in the vicinity of the crack tip that principally results from a dominant bending component of stress. The crack depth relative to specimen width, $\frac{a}{W}$,

needs to be close to 0.5, specifically within the range of $0.45 \leq \frac{a}{W} \leq 0.55$. This choice of crack aspect ratio ensures that both high constraint and suitable K_{Jc} capacity will be achieved. Other specimen types, such as uniaxially loaded center cracked tension panels, surface cracked tension panels, or bend bars with shallow cracks, are not recommended for T_o determinations. These latter specimens suffer loss of constraint at low K_{Jc} levels and are unsuitable to develop a valid, geometry independent K_{Jc} distribution about a mean K_{Jc} of $100\,\text{MPa}\sqrt{m}$. Nevertheless, Standard E 1921 contains one paragraph that allows for specimens that are not suitable for a valid T_o determination. If specimens of an unapproved geometry can be tested at a temperature that develops a K_{Jc} distribution with a mean K_{Jc} of $100\,\text{MPa}\sqrt{m}$, but with unspecified constraint control, that test temperature can be defined as T_Q. However, temperature T_Q is not a provisional value of T_o temperature that can be declared valid by meeting certain other criteria. The two temperatures are likely to be different with T_Q most likely to be low, and therefore, non-conservative relative to T_o [23].

5

Test Equipment

5.1—Compact Specimen Fixtures

THE COMPACT SPECIMENS OF FIG. 7 AND THE DISK SHAPED SPECIMEN of Fig. 8 are loaded using pin and clevis fixturing. The clevis design is shown in Fig. 10. For compact specimens, the load line is offset from the approximate specimen hinge point (located near mid-ligament) by about 3/4W. Hence, the specimen arms rotate open as the load is applied. The small flat surfaces at the bottoms of the clevis holes provide low friction sliding surfaces for the pins as the specimen arms rotate. The direction of sliding is forward, away from the crack tip, so that the starting position for the pins should be to the rear of the holes. Clevises should be made of ultra-high-strength steels such as maraging steel or high quality tool steels. Hardness of the clevis material should be 40 HRC or better. On the other hand, use of clevises made from ultra-high-strength steel is not recommended for pre-cracking, due to the sensitivity of ultra-high strength steels with respect to fatigue crack initiation.

5.2—Bend Bar Fixtures

A schematic description of a bend bar loading fixture is shown in Fig. 11. Again, as with the compact specimen fixture, provision is made for the load bearing pins to slide, outward in this case, during a test. A clip gage is shown attached across the crack mouth, as discussed in paragraph 5.3. A clip gage in this location would normally be used for indicating slow-stable crack growth via autographic methods. This methodology is covered in ASTM Standard E 1820 [24]. All that is necessary for K_{Jc} determinations is a record of the deflection of the top pin versus the applied load in order to determine work done on the specimen for subsequent J-integral calculations.

On the other hand, method E 1921 [19] cites two references that provide ways to use crack-mouth opening displacement to obtain J-integral values. Neither of the two references has been thoroughly validated experimentally. Users of E 1921 should be advised that it would be prudent to first verify the accuracy of such methods before performing a full test series using this option.

Figure 11 shows a clip gage highly exposed such that it could be destroyed on the first test. Cleavage fracture in bend bar specimens of 1T size or larger will cause the release of considerable elastically-stored strain energy, with the broken specimen halves tending to become projectiles. Both the machine operator and the clip gage should be protected. The clip gage can be protected by adding a substantial shroud underneath it for the clip gage to fall into at the time of specimen fracture.

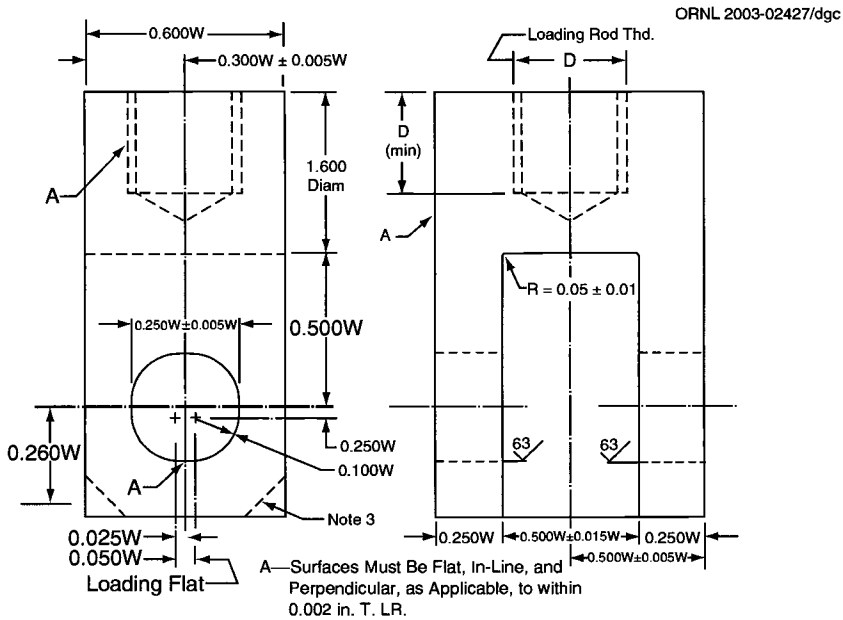

Note 1 – Pin diameter = 0.24 W (+ 0.000 W–0.005 W). For specimens with σ_{ys} > 200 ksi (1379 MPa) the holes in the specimen and in the clevis may be 0.3 W (+0.005 W–0.005 W) and the pin diameter 0.288 W (+0.000 W–0.005 W)
Note 2 – 0.002 in. = 0.051 mm.
Note 3 – Corners of the clevis may be removed if necessary to accommodate the clip gage.

Fig. 10—Clevis design used to test compact specimens. Material used should be high strength steel.

5.3—Clip Gages

Making clip gages such as that shown in Fig. 12 is a feasible venture given reasonable manual skills. However, it is far more practical to purchase commercially available gages. Make or purchase a clip gage of the following characteristics:

1. A linear working displacement range of 5 mm (0.2 in.)
2. Operates in temperatures down to –200°C
3. Self-temperature compensating

For bend bar specimens, load point displacement of the mid-span pin can be measured with a displacement gage that is placed out of the range of the flying specimen halves. Equipment of this type is also available commercially.

5.4—Cryogenic Cooling Chambers

Standard E 1921 offers no specific advice about the equipment to be used for cooling the specimens. Use of liquid baths or use of vaporized gas are both feasible. However, the present document recommends the use of vaporized liquid nitrogen,

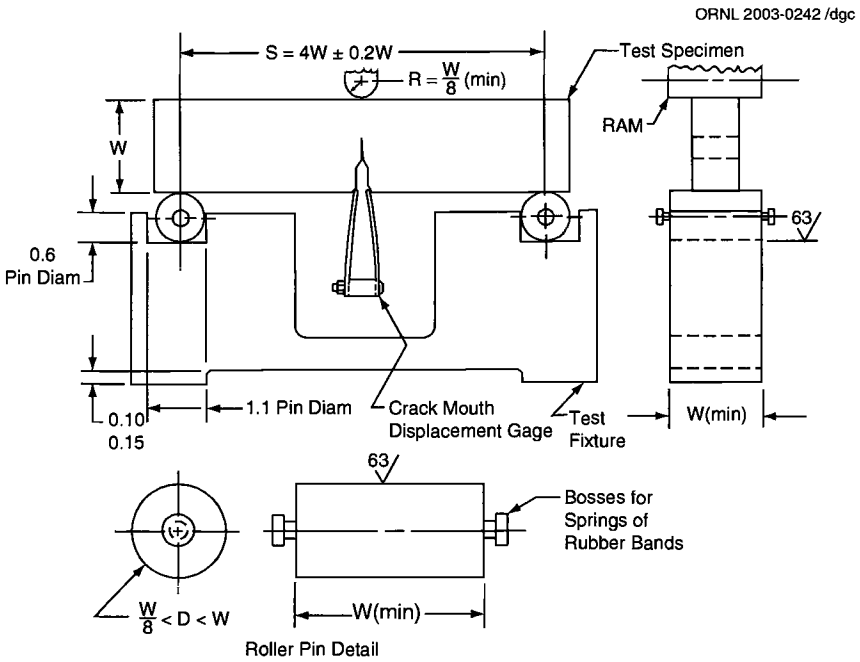

Note 1 – Roller pins and specimen contact surface of loading ram must be parallel to each other within 0.002 *W*.
Note 2 – 0.01 in. = 2.54 mm, 0.15 in. = 3.81 mm.

Fig. 11—Schematic of a typical test fixture for bend specimens, with a specimen in place. Extra equipment needed for safety purposes is not shown.

LN, as the far more practical choice. For this approach, cooling chambers can be anything ranging from cardboard boxes, to Styrofoam containers, to stainless steel furnace boxes, that are otherwise used for low temperature metallurgical precipitation hardening treatments. In all cases, the point of entry for the LN should have a baffle plate to deflect the incoming liquid from impinging directly on the specimens, fixtures, or clip gages. If the cooling chamber is large in comparison to its contents, a fan blade should be inserted to establish uniformity of temperature throughout. Internal ambient temperature can be monitored, but the skin temperature of the specimen should be the focus of control. Thermocouple wires should be spot welded onto the specimen surface or otherwise mechanically attached at the locations indicated in Fig. 13. The duration of transient cooling is dictated by the measured skin temperature of the specimen. The internal temperature of steel specimens will equalize with the skin temperature within a few minutes of reaching a constant skin temperature. The required soak time in E 1921 of 2 min per 10 mm (0.4 in.) of specimen thickness is primarily needed to stabilize the temperature control within the enclosure.

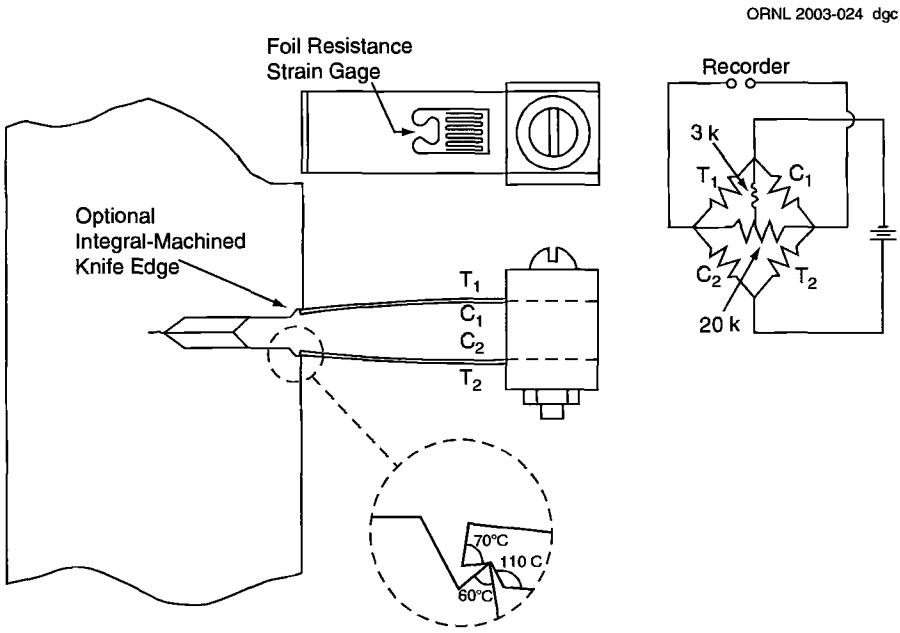

Fig. 12—The most common type of clip gage used in fracture mechanics tests.

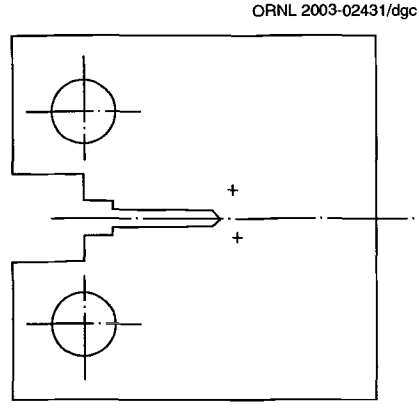

Fig. 13—An approximate suitable location for attaching thermocouple wires. The specimen provides the electrical continuity path between the two thermocouple wires.

6

Pre-Cracking and Side-Grooving of Specimens

6.1—Pre-Cracking

THE CLEVIS DESIGNS OF FIGS. 10 AND 11 ARE ALSO SUITABLE FOR pre-cracking compact specimens, but instead of using ultra high strength steels, use high strength steels with yield strengths in the range of 100–140 ksi. These steels are less sensitive to fatigue crack initiation at sharp corners.

The pre-cracking of specimens is one of the more important operations to be controlled during specimen preparation. The accuracy and distribution of K_{Jc} data could be influenced by warm pre-stress effects, which can result from unsuitable pre-cracking practices. In particular, the pre-cracking requirements stipulated in other ASTM fracture mechanics methods are not suitable for transition range work. Fatigue pre-cracking can be performed at room temperature so long as K_{max} (see Nomenclature) is kept below (20 MPa $\sqrt{m}$). Testing machines that can be operated under load control are preferable for such work. To initiate a fatigue crack from a machined notch, K_{max} of the fatigue cycle can be as high as 27 MPa $\sqrt{m}$ (24.5 Ksi $\sqrt{in}$). Once initiated, a program of periodic gradual load (reduction) should be started to arrive at K_{max} = 20 MPa$\sqrt{m}$ (18 Ksi$\sqrt{in}$) when the fatigue crack is within 0.64 mm (0.025 in.) of the planned endpoint. Strive to keep K_{max} at or below 20 MPa$\sqrt{m}$ for the final 0.64 mm of pre-cracking. The total depth of the fatigue pre-crack should constitute at least 5 % of the initial crack size or, in the case of small specimens, at least 1.25 mm (0.05 in.), whichever is the larger dimension. Use an R ratio of 0.1. See the Nomenclature for definitions.

Pre-cracking of 1T size specimens is expected to take about 1×10^5 to 2×10^5 cycles. On occasion, some steels will be encountered that do not develop fatigue pre-cracks using the above K_{max} levels recommended. In such a case, test the particular steel for crack growth rate using ASTM Standard E 647 [25]. Find the K_{max} level for a crack growth rate of 10^{-6} inches per cycle (at R = 0.1). Then, finish the final 0.64 mm of pre-crack at this K_{max} level. The pre-cracking recommendations of Standard E 1921 have not been stated completely herein, since the pre-cracking provisions are undergoing revisions at the present time.

6.2—Side-Grooving

Side-grooving is not mandatory; however, typical side-groove depths used are 20 or 25 % (10 or 12.5 % each side of the specimen thickness). The optimum included angle of the cutter can be 45°, but up to 90° is considered acceptable. If the experimental plan is to use side-grooves, pre-crack the test specimens before side-grooving. Fatigue cracks are essentially invisible at the root of the machined surface of a side-groove notch.

If the specimen thickness between the side-groove roots is designated B_N, and full thickness is designated B, dimension B_N is used in the calculation of the plastic part of the J-integral. On the other hand, the weakest link size effect expression of Eq 8 uses the ratios of the full thicknesses, B and B_x, for specimens with or without side-grooving.

Side-grooving is believed not to affect the value of K_{Jc} obtained. This statement is only partially true. If K_{Jc} instability is not preceded by slow-stable crack growth, the above statement is, for all intents and purposes, correct. However, if K_{Jc} is preceded by 0.1 mm (0.04 in.) or more of slow-stable crack growth, the truth of the above statement is subject to question. Slow-stable growth begins to be a problem as the test temperature approaches the fully ductile range. Side grooving affects the rate of fracture toughness development with crack growth for K_R-curves [1,26]. See Fig. 14. The solid-line curves in this figure are upper shelf K_R-curves. The data points shown are from specimens that developed K_{Jc} cleavage failures after some prior slow-stable crack growth. The difference in K_{Jc} is tolerable up to about 1 mm of stable-ductile crack growth. For small specimens, such as precracked Charpys, the permissible amount of prior ductile crack growth is up to 5 % of crack size, or 1 mm, whichever is the smaller. This limitation on stable crack growth is a recent modification to the E 1921 standard. Most of the original data used to develop the Master Curve shape were from non-side-grooved specimens, for which the effect of side-grooving on stable growth toughness development was not an issue.

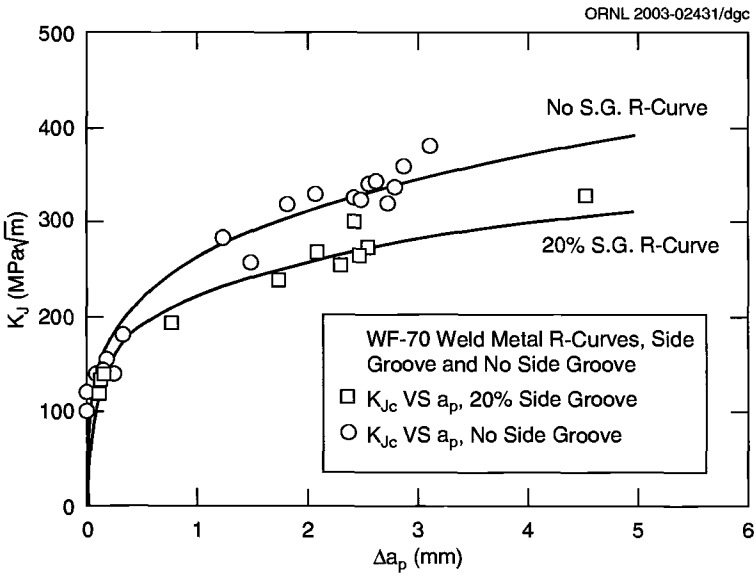

Fig. 14—Effect of side grooving (SG) on fracture toughness development in the presence of slow stable crack growth. The two solid R-curves were developed separately at upper shelf temperature. Data points are K_{Jc} versus Δa_p values, from testing performed in the transition range.

7

Test Practices

THE K_{JC} TOUGHNESS LIMIT VALUE, $K_{JC\ (LIMIT)}$, GIVEN BY EQ 12, WILL almost always occur near the point of maximum load in the test record. To avoid specimen failure due to excessive system crack drive at maximum load and beyond, the applied load must decrease equally with the decrease in load bearing capacity of the test specimen. Hence, the test machine must be operated under rigid displacement control. Servo-hydraulic machines can be displacement controlled, using the feedback voltage of a clip gage attached across either the crack mouth or the load-line of a specimen. An alternative is to use the machine actuator voltage feedback for stroke control. The former approach provides infinitely stiff control, and the latter will contain the slightly softer spring-like compliance of the pull rods and clevises. Screw-driven test machines usually have stiff frames and cross-heads, so they perform the same as a servo-hydraulic machine under stroke control. All of the above approaches have been proven to work successfully, provided that the pull rods are of suitable stiffness.

Fatigue pre-cracking, as discussed in Section 6.1, is most easily performed in servo-hydraulic machines under load control. The post-test fracture surfaces of specimens must be examined to determine the initial machined crack size, the fatigue pre-crack depth, and the slow stable crack growth at the end of the test. The nine-point method of calculating crack depth was discussed in Section 3.3.

As previously mentioned in Section 5.4, thermocouples are attached, either by spot welding or by other mechanical methods, onto one of the specimen surfaces, as illustrated in Fig. 13.

After the thermal soaking period has elapsed, specimens should be loaded slowly since the transition temperature obtained could possibly be influenced by strain rate effects. A good loading rate to select is one for which the value of the $\dot{K}$ in the linear part of the load-displacement record is 100 ± 50 MPa $\sqrt{m}$ per min. The value of $\dot{K}$ will decrease in the nonlinear part of the test record.

The calibration of every piece of equipment used in a test can be checked using the initial linear elastic slope of a test record. Compliance is displacement divided by the load, (V_{LL}/P). Compliance is normalized by multiplying by the elastic modulus and specimen thickness, B, or effective thickness, B_e (see Note 2). For example, the normalized compliance is given by $C_n = E'BV_{LL}/P$. Initial elastic slopes can be generated by pre-cycling specimens two to three times prior to proceeding with the test. Obtain the average value of C_n, and then refer to Eqs A1.9 or A2.10 in Ref. [24]. When the test is over and the initial pre-crack size can be measured visually, calculate the initial crack size using the average value of C_n. If the prediction is more than 0.01W in error, then find the value of E' that would make the prediction accurate. If the most common experimental value of E' is within ± 10 % of 206 820 MPa (30×10^6psi), then confidence can be had that the testing equipment is operating within expected calibration limits. The forgoing is recommended for

checking the operation of test equipment, not as a substitute for any pretest equipment calibration procedures.

Note 2—To calculate the effective thickness, B_e, of side grooved specimens, use:

$$B_e = B_N(2\text{-}B_N/B)$$

8

Fracture Toughness Calculations

THE DEFINITIONS OF THE TERMS USED IN THIS SECTION ARE GIVEN IN THE NOMENCLATURE.

8.1—Calculation of J-Integral

As previously mentioned in connection with Eq 6, fracture toughness is first determined using the elastic-plastic J-integral corresponding to the point of cleavage instability. Then Eq 6 is used to convert the result into units of stress intensity factor. J-integral is separated into two parts, specifically an elastic component and a plastic component:

$$J_c = J_e + J_p \tag{13}$$

8.2—Calculation of J_p

Figure 15 is a schematic representation of a load-displacement test record, subdivided into elastic area, A_e, and plastic area, A_p, components of work done on the specimen. The line that separates the two areas is parallel to the initial elastic loading line and is fitted to pass through the point of crack instability. The plastic component of J is obtained using the following:

$$J_p = \eta_p A_p/(B_N b_o) \tag{14}$$

For compact and disk shaped compact specimens, use:

$$\eta_p = 2 + 0.522\ b_o/W \tag{15}$$

For bend bars, use a constant $\eta_p = 1.9$, which is accurate for $0.45 \leq \frac{a}{W} \leq 0.55$.

8.3—Calculation of J_e

The elastic contribution to work done is calculated directly from the value of the linear elastic-stress intensity factor, K_e,

$$J_e = K_e^2/E' \tag{16}$$

For compact, C (T), and disk shaped compact specimens, DC (T),

$$K_e = [P/(BB_N W)^{1/2}]\ [f\ (\tfrac{a}{W})_{C(T)} \text{ or } f\ (\tfrac{a}{W})_{DC(T)}\} \tag{17}$$

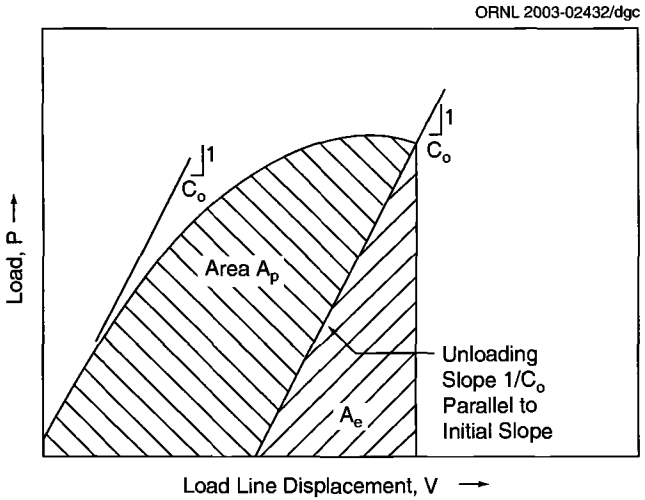

Fig. 15—Areas under a load versus applied load-line displacement plot that represent plastic work done, A_p, and stored elastic strain energy, A_e, at the end of a test.

Crack size, a, is the starting crack length.

For bend specimens,

$$K_e = [PS/[(BB_N)^{1/2} W^{3/2}]] f(\frac{a}{W})_{SE\,(B)} \quad (18)$$

Crack size, a, is the starting crack length.

The equations for $f(\frac{a}{W})$ are given in ASTM method E 1921. Table 4 herein lists values of $f(\frac{a}{W})$ for values of $\frac{a}{W}$ given in increments of 0.01. Linear interpolation between the values given in Table 4 is sufficiently accurate.

TABLE 4—List of $f(\frac{a}{W})$ values for Eqs 17 and 18.

$\frac{a}{W}$	C (T)	DC (T)	SE (B)
0.45	8.339	8.71	9.14
0.46	8.580	8.97	9.42
0.47	8.830	9.25	9.70
0.48	9.093	9.55	10.01
0.49	9.369	9.85	10.32
0.50	9.659	10.17	10.65
0.51	9.964	10.51	11.00
0.52	10.286	10.86	11.36
0.53	10.625	11.24	11.74
0.54	10.984	11.63	12.15
0.55	11.364	12.04	12.57

8.4—Crack Mouth Data

When a crack-mouth opening displacement gage is used instead of a load-line gage, only the J_p calculation is affected. For compact specimens, for which the gage spans the front face at 0.25W in front of the load-line, use [22]:

$$A_p = A_{p(ff)}/1.37 \tag{19}$$

For bend bars having $S = 4W, 0.45 \leq \frac{a}{W} \leq 0.55$, and for which the displacement is measured at the crack mouth, J_p is calculated by replacing A_p in Eq 14 with $A_{p(ff)}$ and using [27]:

$$\eta_{p\,(CMOD)} = 3.785 - 3.1\left(\frac{a}{W}\right) + 2.018\left(\frac{a}{W}\right)^2 \tag{20}$$

For the range of $\frac{a}{W}$ allowed in E 1921, $\eta_{p\,(CMOD)}$ is nominally 2.74, varying by only ± 2 % within that range. The user of Eq 20 would be well advised to confirm the result of using Eq 20, with J_p first determined from one or more load point type test records.

8.5—Units of Measure

The primary units of measure in the Master Curve calculations are as follows:

- K_o and K_{Jc}, MPa $\sqrt{m}$
- E' and σ_{ys}, MPa
- J-Integral, MJ/m²
- Temperature, degrees centigrade, °C
- P, MN
- B and W, meters

The use of the dimensionally consistent metric units given above for calculations of fracture toughness, without the necessity of using internal units-conversion factors, may differ from common practice in the application of ASTM standards related to fracture toughness, but it is much less error-prone. Values of J-integral in MJ/m² may be converted to kJ/m² by multiplying by 1000. Additional convenient conversions are given below.

	Master Curve	Metric Conversions
K_{Jc}	MPa $\sqrt{m}$	kNmm$^{-3/2}$ × 31.62
J	kJ/m²	(kN/mm) × 1000
K_{Jc}	$(E'J)^{1/2}$	E' in GPa (GPa = MPa × 10^{-3})
	Master Curve	English to Metric
K_{Jc}	MPa $\sqrt{m}$	ksi $\sqrt{in}$ × 1.0988
J	kJ/m²	[(in.•lb)/in.²] × 0.175
K_{Jc}	$1.0988(E'J)^{1/2}$	E' in (psi × 10^{-6}) J in (in.•lb)/in.²

9

Determination of Scale Parameter, ($K_o - K_{min}$)

ALL TERMS USED IN THIS SECTION ARE DEFINED IN THE NOMENCLATURE.

9.1—Testing at One Appropriately Selected Test Temperature

The most efficient method of determining a scale parameter is to test six or more specimens at one test temperature and as close as possible to the T_o temperature. A method of making a rough estimate of a test temperature close to T_o is to use data from a Charpy V-notch impact-energy transition curve in conjunction with the following equation:

$$T_{o\ (estimate)} = T_{CVN} + C \tag{21}$$

T_{CVN} is the temperature at which the Charpy energy is optionally either 28 or 41 J. The value of constant C in Eq 21 is a function of the energy choice and test specimen size. See Table 5. The relationship between T_o and $T_{o\ (estimate)}$ is admittedly crude but still adequate for selecting a viable test temperature.

Table 6 lists some example values of $T_{o(estimate)}$ versus experimental results. Values of drop weight NDT transition temperatures [8] are also presented, in case this comparison proves to be of interest.

TABLE 5—Table of offset constants for Eq 21 Charpy V curve estimates of T_o temperature.*

Specimen Size (nT)	Constant C (°C)	
	28 J	41 J
0.4	−32	−38
0.5	−28	−34
1	−18	−24
2	−8	−14
3	−1	−7
4	2	−4

*For pre-cracked Charpy specimens, use C = −50 or −56°C.

TABLE 6—Examples of reference temperatures, T_o, and predictions of T_o from Charpy V curves, plus drop-weight NDT values.

Material	Strength (MPa)		Reference	T_o(°C)	CVN T_{28J} – 18(°C)	Drop-weight NDT(°C)
	σ_{ys}	σ_{UTS}				
Normalized A302B	534	689	ORNL unpublished data	69	68.4	65
Modified A302B (Z7)	476	638	NUREG/CR-6426	–87	–67	–26
SNUPPS weld	528	652	ORNL HSST	–62	–67	–58
A533B Plate 14A	650	820	ORNL heat-treated plate	–44	–20	40
A533B Plate 02	476	628	NUREG/CR–4092	–23	–28	–18
A553B weld 72W	498	606	STP 1046, Vol. 2	–59	–62	–23
A533B weld 73W	490	599	STP 1046, Vol. 2	–62	–69	–34
A533B welds, irradiated	630	730	NUREG/CR-5913	37	6	46
A508 class 2 weld (beltline)	512	613	NUREG/CR-6249	–58	–44	–55
A508 class 2 weld (nozzle)	545	655	NUREG/CR-6249	–32	–44	–50
A508 class 2 weld, irradiated (beltline)	646	747	ORNL/NRC/ LTR-95/18	27	47	...
A508 class 2 weld, irradiated (nozzle)	701	791	ORNL/NRC/ LTR-95/18	62	40	...
A533B HSST Plate 13A	444	600	NUREG/CR-5788	–70	–56	–23
A533B Morland	470	620	NRL-Risley 1006 (R)	–92	–87	–15
20MnMoNi55	450	610	GKSS 93/E/81	–123	–89	...
20MnMoNi55 irradiated	586	...	GKSS 93/E/81	–68	–38	...
CrMoV	660	802	GKSS 93/E/81	60	...	...
A36	250	455	Sorem et al., WRC Bulletin 351	–38	–10	...
A508 class 3	480	635	Iwadate et al., STP 803, Vol. II	–45	–49	...
A470 class 6*	767	870	Iwadate et al., STP 803, Vol. II	–63	–63	...
A508 class 3	456	599	MPC/JSPS-RR, STP 1207	–106	...	–30
A508 class 2	441	...	Macdonald, STP 1114	–46	...	...
A553B heat treated	538	607	Link, STP 1244	–55	–28	4
SM41C	304	461	Ando, Fatigue & Fracture Eng. Mat. Str	–123	...	...
NiCrMo	745	812	Ando, Fatigue & Fracture Eng. Mat. Str	–54	...	...
A508 class 2 heat treated	670	800	NUREG/CR-4249, TSP-3	–20	0	30

*No specimen size adjustment.

9.2—Equations for the Scale Parameter

9.2.1—All Valid Data at One Test Temperature

The following equation was derived using maximum likelihood theory [1]. It is assumed here that:

1. All specimens have been tested at one test temperature.
2. The total number of specimens, N, were of ASTM E 1921 specified geometry.
3. If specimens were of varied sizes, the K_{Jc} values have been converted to a common size (Note 3).
4. All six or more K_{Jc} values are valid. See Section 3.
5. No invalid K_{Jc} data have been discarded.

For the above required conditions, use the following:

$$K_o - K_{min} = \left[\sum_{i=1}^{N}\left(K_{Jc(i)} - K_{min}\right)^4 / N\right]^{1/4} \tag{22}$$

Note 3—To obtain a T_o temperature, the K_{Jc} values must be for, or adjusted to, 25.4-mm (1-in.) equivalent thickness.

9.2.2—Valid Plus Invalid Data at One Test Temperature

The following equation was derived by maximum likelihood theory to use with mixed valid and invalid K_{Jc} data [1]. It is assumed here that:

1. All specimens have been tested at one test temperature.
2. All specimens are of ASTM E 1921 specified geometries.
3. If specimens were of varied sizes, the K_{Jc} values have been converted to one common size. See Note 3.
4. There are at least six valid K_{Jc} values in the mix of valid/invalid data.
5. All invalid data have been censored, i.e., replaced by their dummy K_{Jc} values, as explained below, subsequently size adjusted to 1T equivalence.

An invalid datum replacement (dummy K_{Jc}) value is:

1. The $K_{Jc(limit)}$ value if the K_{Jc} value exceeded the limitation given by Eq 12.
2. K_{Jc} at 1 mm of slow-stable crack growth, when more than 1 mm of stable growth has been measured on the fracture surface.
3. If the point of 1 mm of slow-stable growth cannot be determined, use J_{Ic} [24] converted to K_{Jc} using Eq 6.
4. The smallest dummy K_{Jc} value given by items 1 through 3 shall be used.
5. All dummy values are open to decision on the part of the user. If items 2 through 4 cannot be determined, use the $K_{Jc(limit)}$ value.
6. Size adjust all dummy values to the common 1T specimen size.

Then input all 1T based data, valid and dummy K_{Jc} values, into the following:

$$K_o - K_{min} = \left[\sum_{i=1}^{N}\left(K_{Jc(i)} - K_{min}\right)^4 / r\right]^{1/4} \tag{23}$$

where r is the number of valid data.

10

Determination of Reference Temperature, T_o

10.1—The Single Temperature Method

EQUATION 9 OR EQ 10 CAN BE USED TO SOLVE FOR T_o, GIVEN THAT SCALE parameter ($K_o - K_{min}$) has been determined using either Eq 22 or Eq 23. For all specimens tested at one temperature, T, and all K_{Jc} values are IT size equivalent.

The median K_{Jc} is first calculated using Eq 9.

Given that K_{min} = 20 MPa $\sqrt{m}$, and b = 4:

$$K_{Jc(med)} = 0.9124(K_o - 20) + 20, \quad \text{MPa}\sqrt{m} \tag{24}$$

Equation 10 is rearranged to solve for T_o:

$$T_o = T - \ln[(K_{Jc(med)} - 30)/70]/0.019, \quad °C \tag{25}$$

10.2—The Multi-Temperature Method

Standard E 1921 encourages use of the single-test-temperature method, when such an option is available, since it is the most trouble-free procedure for T_o determinations. The multi-temperature method is available for cases involving transition range data that have been acquired at multiple test temperatures. Reasons for doing so would be to work with historical data sets not necessarily developed with T_o determination in mind, or to experimentally observe the shape of the transition range curve for a specific steel. Conformance to all other rules for data acceptance can result in an equally suitable T_o temperature determination. The following equality was developed, making the assumption that the data follow the Master Curve trend:

$$\sum_{i=1}^{N} \delta_i \frac{\exp[0.019(T_i - T_o)]}{11 + 77\exp[0.019(T_i - T_o)]} = \sum_{i=1}^{N} \frac{(K_{Jc(i)} - 20)^4 \exp[0.019(T_i - T_o)]}{[11 + 77\exp[0.019(T_i - T_o)]]^5} \tag{26}$$

Refer to the Nomenclature for definitions.

The rules applied to the input into Eq 26 are as follows:

1. δ_i is the Kronecker delta. Its use is defined in the Nomenclature.
2. If $K_{Jc(i)}$ exceeds the $K_{Jc(limit)}$ value of Section 3.2, then $K_{Jc(i)}$ is invalid, and $K_{Jc(limit)}$, converted to 1T equivalence, is an eligible replacement dummy value.
3. All $K_{Jc(i)}$ data, valid and invalid dummy values, are adjusted to 1T size equivalence. Use Eq 8 to convert K_{Jc} data of another size to 1T equivalence.
4. The useable test temperature, T_i, range is within $T_o \pm 50°C$.

5. There must be at least six valid $K_{Jc(i)}$ values used to establish the T_o temperature.
6. If Δa_p, described in Section 3.3 exceeds 1 mm, the K_J value at the point of 1 mm ductile crack-growth replaces the invalid $K_{Jc(i)}$ datum.
7. If K_J at Δa_p = 1 mm cannot be determined, an alternate eligible option is dummy K_{Jc} determined from J_{Ic} and Eq 12. See Ref. [24].
8. T_i shall always be in units of °C and K_{Jc} in units of MPa $\sqrt{m}$.
9. All dummy values are open to decision on the part of the user. If items 6 or 7 cannot be determined, use the $K_{Jc(limit)}$ value of item 2.
10. Do not use data outside of the $T_o \pm 50$°C temperature limits. At test temperatures above $T_o + 50$°C, problems can come from intrusion of R-curve effects. Weakest link size effects assumed in the use of Eq 8 will tend to vanish as both upper shelf and lower shelf test temperatures are approached.

It will also become evident to the user of Eq 26 that the approximate T_o temperature is needed before the computational procedure can be executed. For an iteration method, use the Charpy energy curve and Eq 21 to make the first estimate of the true T_o temperature. Then, zero-in on the true T_o using only valid data at first. Continue iterating with valid and invalid data until a majority of the data are within the updated $T_o \pm 50$°C temperature range. Presumably there will be the required six valid $K_{Jc(i)}$ values within that range.

11 Development of Tolerance Bounds

THE ESTABLISHMENT OF TOLERANCE BOUNDS ON DATA SCATTER CAN be accomplished by using one of two available methods. One method uses standard deviations for the data distribution that can be extended to chosen probability levels (tolerance bounds) with the use of standard normal deviates, Z. The other option is to use cumulative probabilities expressed by the Weibull distribution. Because the methods differ from the standpoint of mathematical approach, the tolerance bound curves calculated will differ slightly. Since this difference is small, the choice among the two is optional.

11.1—Standard Deviation Method (E 1921-97)

Standard deviation on data scatter, σ, is a function of the Weibull slope and the median fracture toughness level:

$$\sigma = \theta[\Gamma(1 + 2/b) - \Gamma^2(1 + 1/b)^{1/2} \quad (27)$$

The terms θ and b are scale parameter and Weibull slope, respectively. Accordingly, for Weibull slope, b = 4:

$$\Gamma(1.5) = 0.8862$$

$$\Gamma^2(1.25) = 0.8216$$

Values for gamma functions, Γ, can be found in handbooks of mathematical functions [28]. Substituting $(K_o - K_{min}) = \theta$ and incorporating Eq 9 result in the following standard deviation:

$$\sigma = 0.28\,(K_{Jc(med)} - K_{min}) \quad (28)$$

To set a lower tolerance bound at P_f = o.xx, one could use:

$$K_{Jc(o.xx)} = K_{Jc(med)} - Z_{(o.xx)}\sigma \quad (29)$$

Values of $Z_{(xx)}$ are one tail standard normal deviates. See Table 7. Since the standard deviation is a function of $K_{Jc(med)}$, the Master Curve, Eq 10, can be substituted into Eq 29, resulting in tolerance bound equations of the same form, but with revised coefficients.

$$K_{Jc\,(o.xx)} = D_1 + D_2 \exp[0.019\,(T - T_o)], \quad MPa\sqrt{m} \quad (30)$$

Coefficients D_1 and D_2 are listed in Table 8. For example, the 5 % and 95 % tolerance bounds can be calculated using:

$$K_{Jc(.05)} = 25.4 + 37.8\exp[0.019(T - T_o)], \quad MPa\sqrt{m} \tag{31}$$

$$K_{Jc(.95)} = 34.6 + 102.2\exp[0.019(T - T_o)], \quad MPa\sqrt{m} \tag{32}$$

See Fig. 16.

11.2—Cumulative Probability Method (E 1921-02)

The Weibull cumulative probability approach has one general equation:

$$K_{Jc(o.xx)} = \left[\ln\frac{1}{1 - o.xx}\right]^{1/4}(K_{o\,(T)} - K_{\min}) + K_{\min}, \quad MPa\sqrt{m} \tag{33}$$

Tolerance bounds calculated by Eq 33 require the determination of K_o at every temperature point, T, using Eq 11.

TABLE 7—Standard normal deviates, Z, for one-tail cumulative probabilities.

Tolerance Bound Conf.	
0.XX	Z
0.125	1.15
0.100	1.28
0.075	1.44
0.05	1.64
0.03	1.88
0.01	2.33

TABLE 8—Coefficients for tolerance bounds $K_{Jc\,(xx)}$ = D1 + D2 EXP [0.019 (T-T_o)] MPa $\sqrt{m}$.

TB (xx)	D1	D2
0.01	23.5	24.5
0.02	24.3	30.0
0.03	24.7	33.2
0.04	25.1	35.7
0.05	25.4	37.8
0.10	26.4	44.9
0.90	33.6	95.1
0.95	34.6	102.2
0.96	34.9	104.3
0.97	35.3	106.8
0.98	35.8	110.3
0.99	36.5	115.5

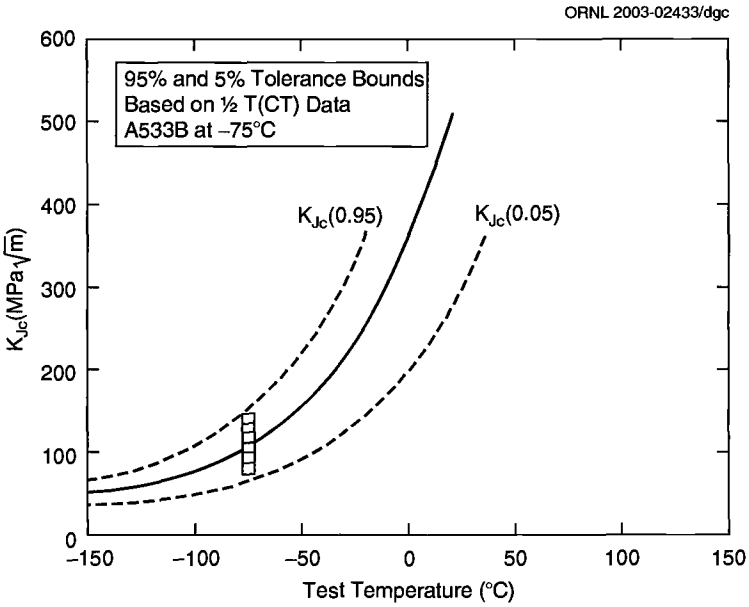

Fig. 16—Six K_{Jc} data values (open squares), the Master Curve determined therefrom and the 95 % and 5 % tolerance bounds on data scatter.

11.3—Margin Adjustment to the T_o Temperature

As discussed in Section 3.1, the selected sample size of six specimens represents a compromise involving a practical number of specimens with acceptable accuracy in the determination of K_o. Hence, it is clear that T_o temperatures obtained using Standard E 1921 will contain some small measure of uncertainty. If this measure of uncertainty is deemed unacceptable, for example in the establishment of lower bound curves, some margin adjustment to T_o can be added. For values of $K_{JC}(med) \geq 83$ MPa $\sqrt{m}$, the following equation can be used:

$$\Delta T_o = \sigma_{T_o} = 18/\sqrt{N}, \quad °C \tag{34}$$

where σ_{To} is one standard deviation on the T_o reference temperature distribution, and N is total data (valid and invalid). When $K_{JC}(med) < 83$ MPa$\sqrt{m}$, slightly larger values of the numerator in Eq 34 are recommended by Ref. [19].

Equation 34 has been formulated using statistical theory, supported with test data [1,29]. The distribution on T_o is two tail, hence the standard normal deviates in Table 9 apply. It is recommended that 85 % confidence should be sufficient.

Usually the compensation for uncertainty in T_o is a temperature adjustment made to tolerance bound curves that underlie the data. See Fig. 17. Such curves that define a lower bound of data scatter are the ones for which safe operating temperature judgments are made when design calculations are applied deterministically.

TABLE 9—Standard normal deviates, Z, for two-tail distributions.	
Percent Conf	Z
75	1.15
80	1.25
85	1.44
90	1.64
95	1.96
98	2.33

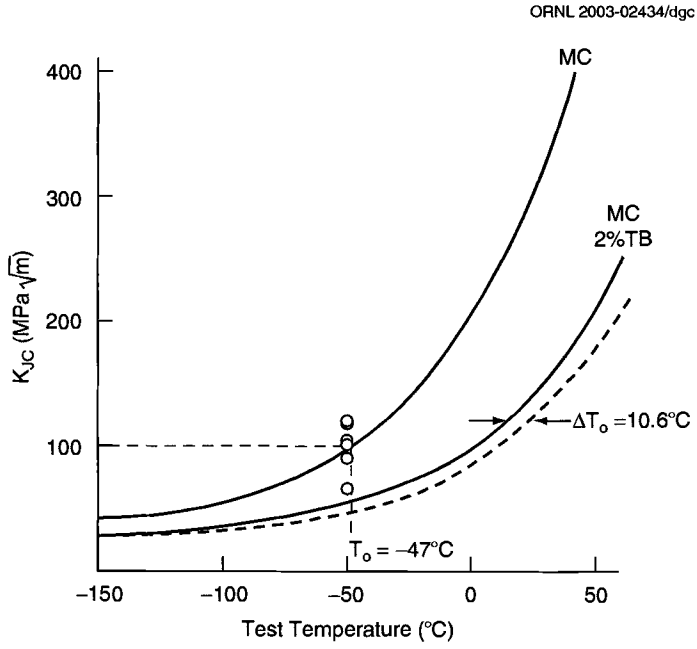

Fig. 17—Margin adjustment (10.6°C) applied to the 2 % tolerance bound of the Master Curve (MC).

12

Concepts Under Study

12.1—Consideration of the Pre-Cracked Charpy Specimen

EVEN THOUGH THE CHARPY (CVN) BEND BAR IS SMALLER THAN ANY other candidate fracture mechanics specimen, it is being considered for use because it is the most common non-fracture mechanics specimen used in manufacturing and engineering applications. Oftentimes this CVN bar is the only fracture toughness type of specimen inserted into the surveillance capsules of nuclear reactor pressure vessels, and in some cases, the important pre-irradiation or baseline CVN transition curves were not developed. Hence, there is good motivation to determine if valid fracture mechanics-based K_{Jc} values can be obtained from the Charpy bar after it has been fatigue pre-cracked into a fracture mechanics configuration. If the effort were successful, it would obviate the need for baseline CVN data to evaluate irradiation damage currently judged by the CVN ΔT curve shift.

The pre-cracked Charpy (PCCV) specimen is a bend bar of 10 × 10 mm (0.4 × 0.4 in.) cross-section that contains a 2-mm (0.079-in.) deep machined notch of 0.25 mm (0.01 in.) root radius [30,31]. Specimens have to be fatigue pre-cracked to about a 5-mm depth to be useful for K_{Jc} determinations. The K_{Jc} capacity of a PCCV specimen, determined using **Eq** 12, is extremely limited, so that the test temperature has to be about 25°C or more below the T_o temperature. The median K_{Jc} has to be about 80MPa $\sqrt{m}$ or lower. At these test temperatures, the lower shelf of fracture toughness is being approached, and consequently the accuracy of T_o determinations is diminished.

One remedy for this situation under consideration is to increase the accuracy of the $K_{Jc(med)}$ determination by increasing the required number of valid data. The following equation establishes the estimated number of smaller specimens required to have equivalent accuracy to that of six 1T size specimens tested at the T_o temperature.

$$N = 6\left[\frac{7}{8}\frac{(K_{Jc\,(med)} - 20)}{(K_{Jc\,(med)} - 30)}\right]^2 \tag{35}$$

$K_{Jc(med)}$ is the median of K_{Jc} data at the selected test temperature, converted to 1T size equivalence. Table 10 shows some example determinations. This manual recommends performing no tests below (T_o – 50°C), since the weakest link-based specimen size effects predicted using **Eq** 8 tend to vanish. Some data have produced lower values of T_o from pre-cracked Charpy specimens than from larger specimens, while other data have produced identical values.

12.2—Dealing with Macroscopically Inhomogeneous Steels

The following is a recommended method for dealing with random macroscopic inhomogeneity, oftentimes found in heavy plate steels (see Note 4). The approach

TABLE 10—Calculated number of specimens to retain accuracy of T_o determinations at low test temperatures.

$K_{Jc\ (med)}$ MPa $\sqrt{m}$	T-T_o °C	No Spec. Required
100 to 84	6.4	6
83 to 66	23.8	7
65 to 58	42.0	8
<58	48.2	...

is to eliminate, from a random sampling plan, the non-conservative data. The result will be a conservative T_o temperature to represent the fracture toughness distribution within the plate. Background information and an additional procedure of value for the HAZ in welds can be found in Ref. [32]. The following evaluation procedure was applied to data from a round robin conducted by The Welding Institute (TWI). There were data from 110 specimens to work with. This initial evaluation, showing the effect of inhomogeneity on data sets, is illustrated in Fig. 18. A plot such as this is only meaningful when there is one specimen size, one test temperature, and extensive replication. If there had been multiple specimen sizes, all data could have been converted to one size using Eq 8. If the plot of the complete data set closely follows the best fit straight line, up to K_{JC}(limit) at M = 30, then the data indicate that there is no problem of inhomogeneity. In the TWI case, a problem was demonstrated because the best fit straight lines for the 62 toughness values without extreme upward scatter (the solid line in Fig. 18) and

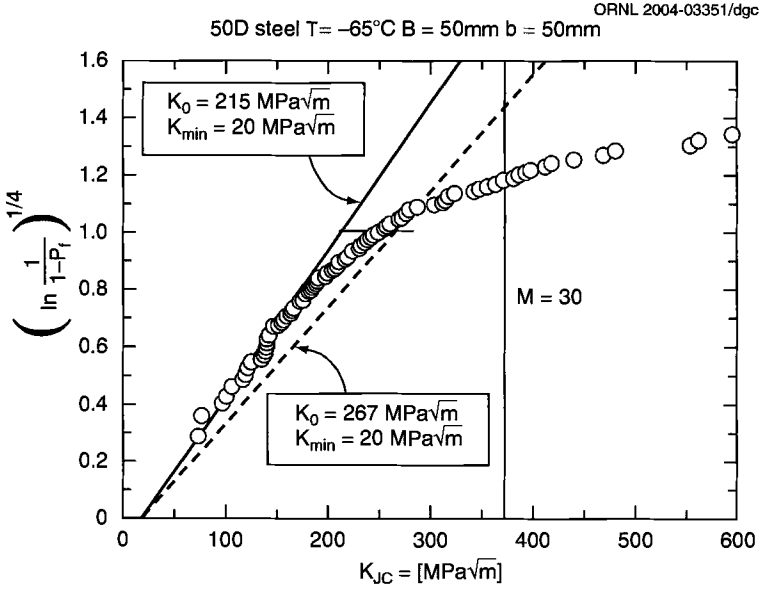

Fig. 18—The Welding Institute round robin fracture toughness data [32]. Including the inhomogeneity makes standard MC analysis non-conservative (267 MPa $\sqrt{m}$ versus 215 MPa $\sqrt{m}$).

for the complete data set (the broken line in Fig. 18) were noticeably different. Furthermore, the plot of the complete data set did not follow a nearly straight line up to M = 30. Therefore, a data treatment procedure was warranted.

Note 4—SINTAP Structural Integrity Assessment Procedure for treatment of Fracture Toughness Data [32].

Development of a plot such as Fig. 18 could require as many as 20–30 randomly distributed replicate tests to make an effective demonstration. The data may be tested for invalidity, but they should not be censored at this point. The data should be ranked, and cumulative probability for fracture values, P_f, should be determined using:

$$P_f = (i - 0.3)/(N + 0.4) \tag{36}$$

Then the corresponding values for the coordinate axes are calculated. A significant departure from linearity prior to M = 30 (as indicated on the abscissa) is clear evidence to proceed with the following data reduction steps.

12.2.1—A Maximum Likelihood Estimate for Random Inhomogeneity

The following can be used on test data generated at varied test temperatures with $T_o \pm 50°C$:

Step 1 Censor all data that are in violation of Eq 12. Replace the censored data with the K_{Jc}-limit values.

Step 2 Convert all data, valid and dummy $K_{Jc(limit)}$ values to IT equivalence Eq 8.

Step 3 Determine the T_o temperature using Eq 26. Use an iterative procedure.

Step 4 Determine K_{CENS}, which is $K_{Jc(med)}$, from T_o in Eq 10. Censor all K_{Jc} data above K_{CENS}. All censored values are set to K_{CENS}.

Step 5 Use the data from Step 4 to determine T_o, again using Eq 26. Compare this T_o temperature to the T_o temperature obtained from Step 3. If T_o from Step 5 is more than 8°C lower than T_o from Step 3, return to Step 4. Iterate to a satisfactory convergence.

Step 6 If less than 12 valid data survive Step 5, then a final conservative lower bound can be determined. If all remaining data are at the same temperature, choose the lowest ranked K_{Jc}. If the remaining data are multiple temperature data, use T_o in Eq 10 and calculate the master curve. See Fig. 19 to select the lowest K_{Jc} value. Then calculate T_o using Eq 25.

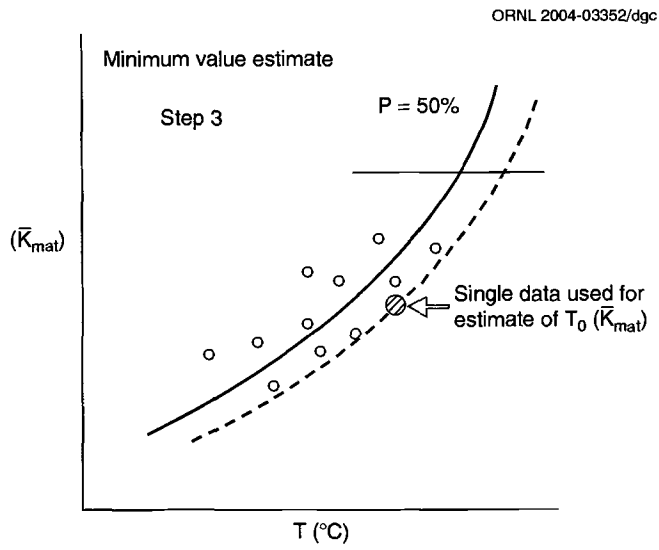

Fig. 19—Principle of SINTAP system 3 analysis (minimum value estimation).

13

Applications

THE MASTER CURVE CONCEPT HAS INTRODUCED TEST PRACTICES AND an analysis methodology that has made fracture mechanics, as applied to structural steels, a practical technology. Specimen size requirements are now practical for routine laboratory testing purposes. Data developed with small specimens can be scaled to predict the fracture toughness behavior in applications that involve other sizes or dimensions. In addition, statistical methods have been introduced that model the data scatter displayed by structural steels in the transition range. Most important, a minimum number of replicate tests is necessary. This allows for the prediction of the lowest fracture toughness likely to be encountered, which is of use to establish design safety margins in terms of critical flaw sizes and/or design stresses.

13.1—Example Applications

Surveillance capsules that are used in nuclear reactors to assess embrittlement damage from neutron bombardment have very limited available space for specimens. Only small specimens are allowable, which heretofore has been a severe handicap for fracture mechanics-type evaluations. With Master Curve practices applied, small and more versatile fracture mechanics type specimens can replace the Charpy V and 1XWOL specimens currently in use.

13.2—Use of Tolerance Bounds

Pressure vessels of the type used in nuclear reactors represent a special problem in fracture toughness evaluations, since cracks embedded in such vessels have the most severe crack-tip constraint. Such constraint is not easily duplicated in test specimens [35]. Hence, the ASME code has sought a resolution in using only lower bound data in the establishment of the K_{Ic} and K_{Ia} design curves [36,37]. The data used to establish these transition temperature design curves required the testing of huge specimens. The Master Curve method employs specimens of the same type, but of considerably smaller size.

The Master Curve represents the ductile-to-brittle transition range characteristic of K_{Ic}-invalid 1-in. (25.4-mm) material thickness. However, the observed specimen size effect can be modeled to scale the data distributions for larger specimens. This scaling is based on the trend of median K_{Jc} values. On the other hand, the statistically predicted 2 % lower tolerance bound on the Master Curve can be shown to reasonably cover the lower bound of data scatter for laboratory specimens of all sizes. Figure 20 shows the specimen size dependence of transition range toughness curves. When size corrected, all of the curves indicate a T_0 temperature close to –87°C. Only the lowest datum in each data distribution is plotted [38]. The vertical curve segments designate the temperature of onset of fully ductile behavior. For all intents and purposes, the lower bound on data scatter is

specimen-size independent, which also includes the ASME favored valid K_{Ic} data. The T_0 reference temperature of the Master Curve has recently been adopted for use in the ASME code for transition temperature indexing of the ASME K_{Ic} curve for data that consist of an accumulation of varied materials obtained from various data sources [36,37].

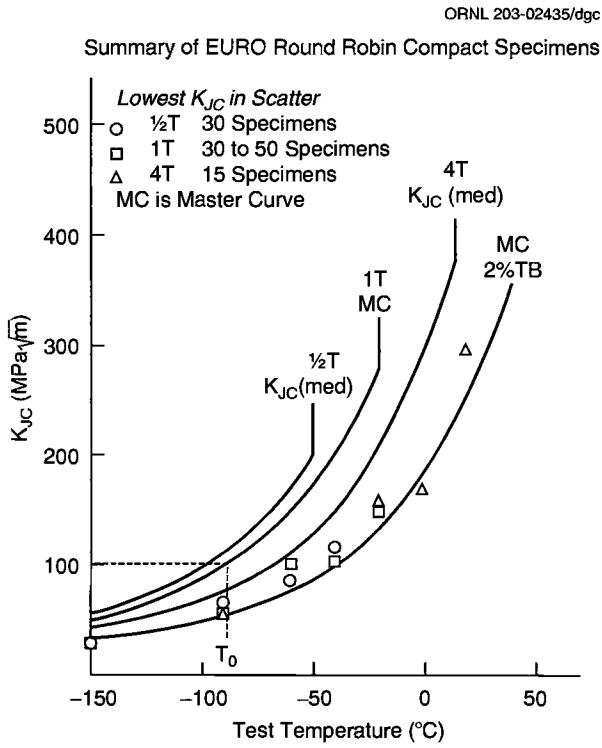

Fig. 20—Calculated transition curves for specimen sizes indicated, based on the 1T Master Curve, for A508, Grade B steel; experimental data shown are the lowest values measured at each test temperature for the specimen sizes tested; temperatures at which fully ductile J-R curve behavior was observed to commence are shown by the vertical curve segments.

13.3—Possible Commercial Applications

Master Curve practices have the potential to be of value in applications where low ambient temperatures can create embrittlement problems with the steels used. The applications that come to mind include:

- Line Pipe
- Offshore Platforms
- Petroleum Storage Tanks
- LNG Tanks
- Ship Plate

- Steel Bridges
- Welded Joints and Steel Frames

ASTM Standard E 1921 recommends that it be considered applicable to steels in the yield strength range of 40–120 ksi. Another requirement is that the fracture mode must be cleavage. Intergranular fracture can lead to a median toughness curve that can fall below the Master Curve as the upper shelf temperature range is approached.

In addition to plate steels, Master Curve testing evaluations can be made on weld metals, specifically, filler metal in weldments. Local brittle zones and heat-affected zones may be special cases not easily adapted to the methodology.

13.4—Application to Other Grades of Steels

Each specimen size selected to define a K_{Jc} data distribution will undergo a mode change to fully ductile behavior at a temperature controlled by specimen size. Fully ductile data with no cleavage fracture are used only as invalid data in the Master Curve analysis procedure, even though such data do not satisfy the six valid K_{Jc} data requirements of Standard E 1921. Therefore, test temperatures should be chosen carefully. For example, ½T size specimens should be tested very near to the T_o temperature. The 1T, 2T, and 4T size specimens can be tested at higher temperatures according to size. Despite this recommendation, it is not necessarily wasteful to test large specimens at test temperatures that are lower than their capacities.

Materials that are of low yield strength may have some difficulty passing the $K_{Jc(limit)}$ requirement when using small specimens. Testing specimens of larger size can be one possible remedy. However, the volume of materials available could also pose a problem. In that case, ASTM Standard E 1820 test practices may be the only alternative available.

Materials that display low Charpy V upper shelf energy have some potential for creating problems. Such materials will display onset of slow-stable crack growth at low applied crack drive, K_J. The crack growth could initiate very near to the T_o temperature, which also indicates that the upper shelf temperature is close by. Larger specimens may help, but in any event, the determination of a T_o temperature for such material may be difficult.

Some steels are brittle at all potential operating temperatures [39,40]. These materials may not scale by specimen size nor necessarily follow any Master Curve-type transition at the intended service temperature. Such data may not be of use for Master Curve-type characterization, but the K_{Jc} values obtained at the expected service temperatures could well be design-useable information.

13.5—Special Design Application Problems

Publication of ASTM Standard E 1921 was the first in a series of steps necessary to make possible the development of fracture control plans for steel structures based directly on fracture toughness measurements made with small laboratory specimens. The advantages of this approach are considerable, both in terms of cost and reliability of the results. However, for design related applications, the shape of the master curve may not always be directly transferable to all geometries.

The median fracture toughness Master Curve is a baseline fracture toughness trend of fracture toughness versus temperature specifically calibrated to 1-in.

thick, through-cracked, laboratory specimens. Therefore, some additional logic potentially could be necessary in order to obtain a physically reasonable ductile to brittle transition fracture toughness representation for the application. First, it is not completely known just how far the weakest link size effect model can be extended outside of the specimen size range covered in experiments. Secondly, in applications, the level of constraint in test specimens may not match the level of constraint in the application. The magnitude of constraint in the application and its impact on fracture toughness properties, for geometries that are known to have steep stress gradients and biaxial stress effects, is not well known at the present time. Research on constraint effects in general is a separate and ongoing activity at the present time. Both problems can be avoided by applying the current concept of a size-independent, lower bound, limiting value of fracture toughness. This experimental approach is still the basis for most, if not all, present ASME codified fracture control procedures [7,9,10]. A straightforward mathematical procedure is available for calculating K_{Ic}, specifically developed for nuclear reactor vessel analyses, from Master Curve data [35].

If the flaws to be considered for analysis are hypothetical, their shape, size, and location need to be carefully chosen with due regard to the historical fact that structural failures are, at times, caused by relatively rare phenomena, often unanticipated or not detectable by inspection. If the application method is to be codified, both thorough discussions and compromise will be needed to produce a logical and long lasting procedure.

The choice of a hypothetical flaw geometry must consider possible in-service creation and growth of flaws due to interactions of stress and environment as well as the possible development of flaws during fabrication. Small flaws which formed and extended by stress-corrosion cracking and/or corrosion-fatigue have occurred in boiling water nuclear reactor pressure vessels [42–44], and at least one such flaw developed in an uninspectable location in an aging eye-bar suspension bridge, leading to its failure [39,40]. All were surface flaws.

Stress analysis is the third key aspect of a fracture control plan. Stresses due to applied loads can be calculated to almost any degree of accuracy, but residual stresses, if present, are harder to quantify. If a structure is capable of reaching limit load before fracture, residual stresses will dissipate and become unimportant. But if the toughness is low, residual stresses will be additive to load-induced stresses in a fracture analysis.

Several major activities are currently underway in Europe and in the United States to develop codified procedures for directly applying Master Curve data. So far, they use the concept of K_{Ic} with a T_0-based reference temperature [36,37], but other hypotheses are being considered. Comprehensive experimental data will be necessary to validate any proposed procedure.

References

[1] Merkle, J. G., Wallin, K., and McCabe, D. E., "Technical Basis for an ASTM Standard on Determining the Reference Temperature, T_o, for Ferritic Steels in the Transition Range," NUREG/CR-5504, Oak Ridge National Laboratory, Oak Ridge, TN, November 1998.

[2] BS5762 "Methods for Crack Opening Displacement (COD) Testing: The British Standards Institution," 1979.

[3] Rice, J. R., Paris, P. C., and Merkle, J. G., "Some Further Results of J-Integral Analysis," *Progress in Flaw Growth and Fracture Toughness Testing, ASTM STP 536*, ASTM International, West Conshohocken, PA, 1973, pp. 231–245.

[4] ASTM Standard E 1152-95, "Standard Test Method for Determining J-R Curves," *Annual Book of ASTM Standards*, Vol. 03.01, ASTM International, West Conshohocken, PA, 1996.

[5] ASTM Standard E 813-89 "Standard Test Method for J_{IC}, a Measure of Fracture Toughness," *Annual Book of ASTM Standards*, Vol. 03.01, ASTM International, West Conshohocken, PA, 1996.

[6] ASTM Standard E 399-90, "Standard Test Method for Plane-Strain Fracture Toughness of Metallic Materials," *Annual Book of ASTM Standards*, Vol., 03.01, ASTM International, West Conshohocken, PA, 1998.

[7] Welding Research Council, "PVRC Recommendations on Toughness Requirements for Ferritic Materials," *WRC Bulletin 175*, 1972.

[8] ASTM Standard E 208-95, "Standard Test Method for Conducting Drop-Weight Test to Determine Nil-Ductility Transition Temperature of Ferritic Steels," *Annual Book of ASTM Standards*, Vol. 03.01, ASTM International, West Conshohocken, PA, 1998.

[9] "Rules for Construction of Nuclear Power Plant Components," ASME Boiler and Pressure Vessel Code, Section III, Division 1, ASME NY, 2001.

[10] "Rules for In-Service Inspection of Nuclear Power Plant Components," ASME Boiler and Pressure Vessel Code, Section XI, ASME NY, 2001.

[11] "Alternative Reference Fracture Toughness for Development of P-T Limit Curves," ASME Boiler and Pressure Vessel Code, Code Case N640, Section XI, Division I, American Society of Mechanical Engineers, February 26, 1999.

[12] Landes, J. D. and Shaffer, D. H., "Statistical Characterization of Fracture in the Transition Region," *ASTM STP 700*, ASTM International, West Conshohocken, PA, 1980, pp. 368–382.

[13] Wallin, K., "Fracture Toughness Transition Curve Shape for Ferritic Structural Steels," *Proceedings of the Joint FEFG/ICF International Conference on Fracture of Engineering Materials and Structures*, 1991, pp. 83–88.

[14] Irwin, G. R., "The Effect of Size Upon Fracturing," *Effect of Temperature on the Brittle Behavior of Metals with Particular Reference to Low Temperatures, ASTM STP 158*, ASTM International, West Conshohocken, PA, 1954, pp. 176–194.

[15] Heerens, J., Read, D. T., Cornec, A., and Schwalbe, K. H., "Interpretation of Fracture Toughness in the Ductile to Brittle Transition Region by Fractographic Observations," ESIS/EGF9, 1991, pp. 659–678.

[16] Landes, J. D. and McCabe, D. E., "Effect of Section Size on Transition Temperature Behavior of Structural Steel," *ASTM STP 833*, ASTM International, West Conshohocken, PA, 1984, pp. 378–392.

[17] Wallin, K., "The Scatter in K_{IC} Results," *Engineering Fracture Mechanics*, Vol. 19, No. 6, 1984, pp. 1085–1093.

[18] Van Der Sluys, W. A. and Miglin, M. T., "Results of MPC/JSPS Cooperative Testing Program in the Brittle-to-Ductile Transition Region," *Fracture Mechanics, ASTM STP 1207*, ASTM International, West Conshohocken, PA, 1994, pp. 308–324.

[19] ASTM Standard E 1921-03, "Standard Test Method for Determination of Reference Temperature, T_o, for Ferritic Steels in the Transition Range," *Annual Book of ASTM Standards*, Vol. 03.01, ASTM International, West Conshohocken, PA, 1998.

[20] Wallin, K., "Master Curve Analysis of Ductile to Brittle Transition Region Fracture Toughness Round Robin Data (The EURO Fracture Toughness Curve)," VTT Publications 367, Espoo Finland, 1998.

[21] Saxena, A., "Nonlinear Fracture Mechanics for Engineers," CRC Press LLC, 1998.

[22] Landes, J. D., "J Calculation from Front Face Displacement Measurements of a Compact Specimen," *International Journal of Fracture*, Vol. 16, R 183–86, 1980.

[23] McAfee, W. J., Williams, P. T., Bass, B. R., and McCabe, D. E., "An Investigation of Shallow-Flaw Effects on the Master Curve Indexing Parameter (T_o) in RPV Material," ORNL/NRC/LTR-99/28, Oak Ridge National Laboratory, Oak Ridge, TN, April 2000.

[24] ASTM Standard E 1820-01 "Test Method for Measurement of Fracture Toughness," *Annual Book of ASTM Standards*, Vol. 03.01, ASTM International, West Conshohocken, PA, 1998.

[25] ASTM Standard E 647, "Test Method for Measurement of Fatigue Crack Growth Rates," *Annual Book of ASTM Standards*, Vol. 03.01, ASTM International, West Conshohocken, PA, 1998.

[26] McCabe, D. E. and Sokolov, M. A., "Experimental Validation Work to Prove the Master Curve Concept," *Fracture, Fatigue, and Weld Residual Stress*, PVP, Vol. 393, ASME, August 1999, pp. 29–34.

[27] Kirk, M. T. and Dodds, R. H., "J and CTOD Estimation Equations for Shallow Cracks in Single Edge Notch Bend Specimens," Nuclear Regulatory Commission, NUREG/CR 5969, UILU-ENG-91-2013, July 1993.

[28] Burington, R. S., *Handbook of Mathematical Tables and Formulas*, 3rd ed., Handbook Publishers Inc., Sandusky, Ohio, 1949.

[29] Wallin, K. "Recommendations for the Application of Fracture Toughness Data for Structural Integrity Assessments," *Proceedings of the IAEA/CSNI Specialists Meeting on Fracture Mechanics Verification by Large Scale Testing*, NUREG/CP 0131, Oak Ridge National Laboratory, Oak Ridge, TN, 1992.

[30] ASTM Standard E 23-96, "Standard Test Methods for Notched Bar Impact Testing of Metallic Materials," *Annual Book of ASTM Standards*, Vol. 03.01, ASTM International, West Conshohocken, PA, 1998.

[31] ASTM Standard E 812-97, "Standard Test Method for Crack Strength of Slow-Bend Pre-Cracked Charpy Specimens of High-Strength Metallic Materials," *Annual Book ASTM Standards*, Vol. 03.01, ASTM of International, West Conshohocken, PA, 2001.

[32] Wallin, K., Nevassmaa, P., Laukkanen, A., and Planman, T., "Master Curve Analysis of Inhomogeneous Ferritic Steels," VTT Industrial System, 17th International Conference on Offshore Mechanics and Arctic Engineering, ASME, OMAE-98-2053.

[33] McAfee, W. J., McCabe, D. E., and Bass, B. R., "A Linearized Least Squares Equation for Calculating T_o," ORNL/NRC/LTR-99/17, Oak Ridge National Laboratory, Oak Ridge, TN, April 2000.

[34] Chaudi, R., "Fracture Toughness Measurements in the Transition Regime Using Small Size Specimens," *Small Specimen Test Techniques, ASTM STP 1329*, 1998, pp. 214–237.

[35] Merkle, J. G., Sokolov, M. A., Nanstad, R. K., and McCabe, D. E., "Statistical Representation of Valid K_{IC} Data for Irradiated RPV Steels," ORNL/NRC/LTR-01/08, Oak Ridge National Laboratory, Oak Ridge, TN, August 2002.

[36] "Use of Fracture Toughness Test Data to Establish Reference Temperature for Pressure Retaining Materials," *ASME Boiler and Pressure Vessel Code: An American National Standard*, Code Case N-629, Section XI, Division 1, American Society of Mechanical Engineers, New York, May 7, 1999.

[37] "Use of Fracture Toughness Test Data to Establish Reference Temperature for Pressure Retaining Materials Other than Bolting for Class 1 Vessels," *ASME Boiler and Pressure Vessel Code: An American National Standard*, Code Case N-631, Section III, Division 1, American Society of Mechanical Engineers, New York, September 24, 1999.

[38] Heerens, J. and Hellman, D., "The Determination of the EURO Fracture Toughness Dataset," submitted to *Engineering Fracture Mechanics*.

[39] NTSB Investigation Team, "Collapse of U.S. 35 Highway Bridge, Point Pleasant, West Virginia, December 15, 1967," National Transportation Safety Board, Department of Transportation, Washington, DC 20591, October 4, 1968.

[40] NTSB Investigation Team, "Highway Accident Report: Collapse of U.S. 35 Highway Bridge, Point Pleasant, West Virginia, December 15, 1967," Final Report, NTSB-HAR-71-1, National Transportation Safety Board, Department of Transportation, Washington, DC 20591, December 16, 1970.

[41] Scheffey, C. F., "Pt. Pleasant Bridge Collapse," *Civil Engineering*, July 1971, pp. 41–45.

[42] Kondo, T., Nakajima, H., and Nagasaki, R., "Metallographic Investigation of the Cladding Failure in the Pressure Vessel of a BWR," *Nuclear Engineering and Design*, Vol. 16, 1971, pp. 205–222.

[43] "Vessel Head Cracking," Attachment #10, *Minutes of ASME Section XI Working Group on Flaw Evaluation*, Nashville, TN, May 15, 1990.

[44] Ranganath, S., "Update on Vessel Head Cracking," Attachment #10, *Minutes of ASME Section XI Working Group on Flaw Evaluation*, Nashville, TN, May 15, 1990.

E 1921 Appendix

(Nonmandatory Information copied directly from appendixes in E1921)

X1. WEIBULL FITTING OF DATA

X1.1 *Description of the Weibull Model*:

X1.1.1 The three-parameter Weibull model is used to fit the relationship between K_{Jc} and the cumulative probability for failure, p_f. The term p_f is the probability for failure at or before K_{Jc} for an arbitrarily chosen specimen from the population of specimens. This can be calculated from the following:

$$P_f = 1 - exp\ \{-[(K_{Jc}-K_{min})/(K_o-K_{min})]^b\} \quad \text{(X1.1)}$$

X1.1.2 Ferritic steels of yield strengths ranging from 275 to 825 MPa (40 to 120 ksi) will have fracture toughness distributions of nearly the same shape when K_{min} is set at 20 MPa$\sqrt{m}$ (18.2 ksi$\sqrt{in.}$). This shape is defined by the Weibull exponent, b, which is constant at 4. Scale parameter, K_o, is a data-fitting parameter. The procedure is described in X1.2.

X1.2 *Determination of Scale Parameter, K_o, and Median K_{Jc}*—The following example illustrates the use of 10.2.1. The data came from tests that used 4T compact specimens of A533 grade B steel tested at −75°C. All data are valid and the chosen equivalent specimen size for analysis will be 1T.

Rank (i)	$K_{Jc(4T)}$ (MPa$\sqrt{m}$)	$K_{Jc(1T)}$ Equivalent (MPa$\sqrt{m}$)
1	59.1	75.3
2	68.3	88.3
3	77.9	101.9
4	97.9	130.2
5	100.9	134.4
6	112.4	150.7

$$K_{o(1T)} = \left[\sum_{i=1}^{N} \frac{\left(K_{Jc(i)} - 20\right)^4}{N}\right]^{1/4} + 20 \quad \text{(X1.2)}$$

$$N = 6$$

$$K_{o(1T)} = 123.4\ \text{MPa}\sqrt{m}$$

X1.2.1 Median K_{Jc} is obtained as follows:

$$K_{Jc(med)} = 20 + (K_{o(1T)} - 20)(0.9124) \text{ MPa}\sqrt{\text{m}} \quad \text{(X1.3)}$$

$$= 114.4 \text{ MPa}\sqrt{\text{m}}$$

X1.2.2

$$T_o = T - \left(\frac{1}{0.019}\right) ln\left[\frac{K_{Jc(med)} - 30}{70}\right] \quad \text{(X1.4)}$$

$$= -85°C$$

X1.3 *Data Censoring Using the Maximum Likelihood Method*:

X1.3.1 *Censoring When $K_{Jc(limit)}$ is Violated*—The following example uses 10.2.2 where all tests have been made at one test temperature. The example data set is artificially generated for a material that has a T_o reference temperature of 0°C. Two specimen sizes are 1/2T and 1T with six specimens of each size. Invalid K_{Jc} values and their dummy replacement $K_{Jc(limit)}$ values will be within parentheses.

X1.3.2 The data distribution is developed with the following assumptions:

Material yield strength = 482 MPa or 70 ksi
T_o temperature = 0°C
Test temperature = 38°C
1/2T and 1T specimens; all a/W = 0.5

X1.3.3 $K_{Jc(limit)}$ values in MPa$\sqrt{\text{m}}$ from Eq. 1.

	0.5T	1T
Specimen size	206	291
1T equivalent	176	291

X1.3.4 *Simulated Data Set*:

Raw Data (K_{Jc}, MPa$\sqrt{\text{m}}$)		Size Adjusted ($K_{Jc(1T)}$, MPa$\sqrt{\text{m}}$)	
1/2T	1T	1/2T [A]	1T
138.8	119.9	119.9	119.9
171.8	147.6	147.6	147.6
195.2	167.3	167.3	167.3
(216.2)	185.0	(176)	185.0
(238.5)	203.7	(176)	203.7
(268.3)	228.8	(176)	228.8

[A] $K_{Jc(1T)} = (K_{Jc(0.5T)} - 20)\ (1/2\ /\ 1)^{1/4} + 20$ MPa$\sqrt{\text{m}}$

$$K_{o(1T)} = \left[\sum_{i=1}^{N} \frac{(K_{Jc(i)} - 20)^4}{r}\right]^{1/4} + 20 \quad \text{(X1.5)}$$

where:

N = 12,
r = 9,
$K_{o(1T)}$ = 188 MPa$\sqrt{m}$,
$K_{Jc(med)}$ = 174 MPa$\sqrt{m}$, and
T_o = 0°C.

X1.3.5 *Censoring When* $\Delta a_p \leq 0.05(W - a_p)$, *not to Exceed 1 mm Limit is Violated*—The following example uses 10.2.2 where all tests have been made at a single test temperature of 38°C. Assume that the test material has properties as defined in X1.3.2 and toughness data as defined in X1.3.4. However, for this example assume that the steel has a low upper shelf. The crack growth limit (see 8.9.2) is 0.64 mm and 1 mm for 0.5T and 1T specimen respectively. The K_J value after 0.64 mm of slow-stable growth is only 197 MPa$\sqrt{m}$ and after 1 mm of slow-stable growth is only 202 MPa$\sqrt{m}$. Therefore, the crack growth limit controls all censoring. The K_J–R curve is specimen size independent so that both 0.5T and 1T specimens will have censored data. In this case the dummy replacement value as per 10.2.2 is the highest ranked valid K_{Jc} value.

Raw Data				1T Size Adjusted Data	
0.5T		1T		0.5T [A]	1T
Δa_p, mm	K_{Jc}, Mpa$\sqrt{m}$	Δa_p, mm	K_{Jc}, Mpa$\sqrt{m}$	K_{Jc}, Mpa$\sqrt{m}$	
0.00	138.8	0.00	119.9	119.9	119.9
0.25	171.8	0.15	147.6	147.6	147.6
0.50	195.2	0.20	167.3	167.3	167.3
0.67	(216.2)	0.55	185.0	(167.3)	185
0.70	(238.5)	1.10	(203.7)	(167.3)	(185)
0.71	(268.3)	1.15	(228.8)	(167.3)	(185)

[A] $K_{Jc(1T)} = K_{Jc(0.5T)} - 20) \bullet (0.5 / 1)^{1/4} + 20$ Mpa$\sqrt{m}$

$$K_{o(1T)} = \left[\sum_{i=1}^{N} \frac{(K_{Jc(i)} - 20)^4}{r} \right]^{1/4} + 20 \qquad \text{(X1.6)}$$

where:

N = 12,
r = 7,
$K_{o(1T)}$ = 186 MPa$\sqrt{m}$,
$K_{Jc(med)}$ = 171 MPa$\sqrt{m}$, and
T_o = 1°C.

X2. MASTER CURVE FIT TO DATA

X2.1 ***Select Test Temperature*** (see 8.4):
X2.1.1 Six 1/2*T* compact specimens,
X2.1.2 A 533 grade B base metal, and
X2.1.3 Test temperature, T = –75°C.
X2.2 In this data set, there are no censored data.

Rank (*i*)	$K_{Jc(1/2T)}$ (MPa$\sqrt{m}$)	$K_{Jc(1T)}$ Equivalent (MPa$\sqrt{m}$)
1	91.4	80.0
2	103.1	89.9
3	120.3	104.3
4	133.5	115.4
5	144.4	124.6
6	164.0	141.1

X2.3 *Determine* K_o *using* Eq. X1.2:

$$K_{o(1T)} = 115.8 \text{ MPa}\sqrt{m}, \text{ and}$$

$$K_{Jc(med)} = [\ln(2)]^{1/4} (K_o - 20) + 20 = 107.4 \text{ MPa}\sqrt{m}.$$

X2.4 *Position Master Curve*:

$$T_o = T - (0.019)^{-1} \ln[K_{Jc(med)} - 30)/70] \quad \text{(X2.1)}$$

$$= -75 - ln[(108.5-30)/70]/0.019 = -80°C.$$

X2.5 *Master Curve*:

$$K_{Jc(med)} = 30 + 70 \exp [0.019(T + 80)] \quad \text{(X2.2)}$$

X2.5.1 See Fig. X2.1.

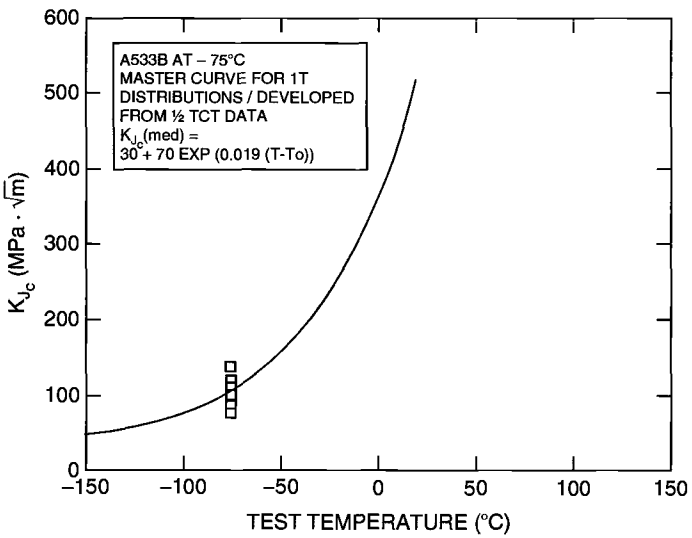

Note 1—Toughness data are converted to 1T equivalence.

Fig. X2.1—Master Curve for 1T Specimens Based on 1/2 *T* Data Tabulated in Step X2.2

X3. EXAMPLE MULTITEMPERATURE T_o DETERMINATION

X3.1 *Material:*
A533 Grade B plate
Quenched and tempered
900°C WQ; and 440°C (5 h) temper

X3.2 *Mechanical Properties:*
Yield strength: 641 MPa (93 ksi)
Tensile strength: 870 MPa (117.5 ksi)
Charpy V:
28-J temperature = –5°C (23°F)
41-J temperature = 16°C (61°F)
NDT: 41°C (106°F)

X3.3 K_{Jc} *Limit Values:*
Specimen Types:
1/2T C(T) with $a_o/W = 0.5$
1T SE(B) with $a_o/W = 0.5$

Test Temperature (°C)	Yield Strength (MPa)	$K_{Jc(limit)}$ (MPa$\sqrt{m}$)	
		1/2T	1T
–10	651	239	338
–5	649	238	337
0	648	238	337
23	641	237	335

X3.4 *Slow-stable Crack Growth Limits:*

$$K_{Jc(1\ mm)} = 263\ \text{MPa}\ \sqrt{\text{m}}\ \text{for 1T SE}(B)\ \textit{specimen};$$

$$K_{Jc(0.64\ mm)} = 255\ \text{MPa}\ \sqrt{\text{m}}\ \text{for 1/2T C}(T)\ \textit{specimen}$$

X3.5 *Estimation Procedure #1 from Charpy Curve:*

$$T_{o(est)} = T_{28J} + C = -5° - 18° = -23°C$$

$$T_{o(est)} = T_{41J} + C = 16° - 24° = -8°C$$

Conduct four 1T SE(B) tests at –20°C.

X3.6 T_o *Estimation Procedure #2 from Results of First Four Tests:*

First four tests at –20°C:

K_{Jc}, MPa$\sqrt{\text{m}}$
135.1
108.9
177.1
141.7

Calculate preliminary $T_{o(est)\#2}$ from data to determine allowable test temperature range:

$$K_{Jc(med)} = 137\ MPa\sqrt{m};$$

$$T_{o(est)\#2} = -42°C$$

Estimated temperature range or usable data:

$$= T_{o(est)\#2} \pm 50°C$$

$$= -92°C < T_i < +8°C$$

Now conduct additional testing within this range for T_o determination.

X3.7 *Calculation of T_o (Eq. 23):*

Use data between –92°C and 8°C based on $T_{o(est)\#2}$

$$T_o = -48°C$$

The valid test temeprature range is –98°C to 2°C. Original claculations were performed with data in this regime. Therefore, no iteration is required.

X3.8 *Qualified Data Summation:*

$(T - T_o)$ Range (°C)	Number of Valid Tests, r_i	Weight Factor, n_i	$r_i \cdot n_i$
50 to –14	43	1/6	7.2
–15 to –35	5	1/7	0.7
–36 to –50	0	1/8	0

Validity check:

$$\Sigma r_i n_i = 7.9 > 1.0$$

TABLE X3.1—Data tabulation.

Test Temperature, (°C)	Specimen		K_{Jc} (MPa$\sqrt{m}$)		δ_j
	Type	Size	Raw Data	1T Equivalent	
–130	C(T)	1/2T	59.5	53.2	1
			85.1	74.7	1
			55.3	49.7	1
			56.4	50.6	1
–80	C(T)	1/2T	51.3	46.3	1
			87.9	77.1	1
			113.4	98.5	1
–65	SE(B)	1T	73.9	73.9	1
			126.8	126.8	1
–55	C(T)	1/2T	167.7	144.2	1
			88.5	77.6	1
			115.2	100.0	1
			81.4	71.6	1

TABLE X3.1—Data Tabulation—*Continued*

Test Temperature, (°C)	Specimen		K_{Jc} (MPa$\sqrt{m}$)		δ_j
	Type	Size	Raw Data	1T Equivalent	
			121.9	105.7	1
			145.0	125.1	1
			104.2	90.8	1
			64.4	57.3	1
			96.8	84.6	1
			114.5	99.5	1
			107.4	93.5	1
			81.0	71.3	1
			70.0	62.0	1
			131.8	114.0	1
			69.5	61.6	1
			67.5	59.9	1
–30	C(T)	1/2T	102.3	89.2	1
			194.0	166.3	1
			170.4	146.5	1
			129.5	112.1	1
			118.2	102.6	1
			147.9	127.5	1
			178.8	153.5	1
			95.9	83.8	1
–20	SE(B)	1T	135.1	135.1	1
			108.9	108.9	1
			177.1	177.1	1
			141.7	141.7	1
			174.4	174.4	1
			84.8	84.8	1
			132.1	132.1	1
–10	C(T)	1/2T	211.4	180.9	1
			179.9	154.5	1
			171.8	147.6	1
			153.0	131.8	1
			236.9	(204)	0
			156.8	135	1
–5	C(T)	1/2T	121.5	105.3	1
			194.2	166.5	1
			110.4	96.0	1
			197.0	168.8	1
			134.7	116.5	1
			264.4	(203)	0
0	C(T)	1/2T	277.8	(198.9)	0
			218.9	187.2	1
			107.7	93.7	1
			269.3	(203)	0
			327.1	(203)	0
23	C(T)	1/2T	325 [A]	(202)	0
			328 [A]	(202)	0
			227	194	1

[A] R-curve (no cleavage instability).

X4. CALCULATION OF TOLERANCE BOUNDS

X4.1 The standard deviation of the fitted Weibull distribution is a mathematical function of Weibull slope, $K_{Jc(med)}$, and K_{min}, and because two of these are constant values, the standard deviation is easily determined. Specifically, with slope b of 4 and K_{min} = 20 MPa$\sqrt{m}$, standard deviation is defined by the following **(24)**:

$$\sigma = 0.28\, K_{Jc\ (med)}[1-20/K_{Jc(med)}] \tag{X4.1}$$

X4.1.1 *Tolerance Bounds*—Both upper and lower tolerance bounds can be calculated using the following equation:

$$K_{Jc(0.xx)} = 20 + \left[ln\left(\frac{1}{1-0.xx}\right)\right]^{1/4}\{11 + 77\exp[0.019(T-To)]\} \tag{X4.2}$$

where temperature "T" is the independent variable of the equation; xx represents the selected cumulative probability level; for example, for 2% tolerance bound, $0.xx$ = 0.02. As an example, the 5 and 95% bounds on the Appendix X2 master curve are:

$$K_{Jc(0.05)} = 25.2 + 36.6\exp[0.019\,(T + 80)] \tag{X4.3}$$

$$K_{Jc(0.95)} = 34.5 + 101.3\exp[0.019\,(T + 80)]$$

X4.1.2 The potential error due to finite sample size can be considered, in terms of T_o, by calculating a margin adjustment, as described in X4.2.

X4.2 *Margin Adjustment*—The margin adjustment is an upward temperature shift of the tolerance bound curve, Eq. X4.3. Margin is added to cover the uncertainty in T_o that is associated with the use of only a few specimens to establish T_o. The standard deviation on the estimate on T_o is given by:

$$\sigma = \beta/\sqrt{r}\ (°C), \tag{X4.4}$$

where:

r = total number of specimens used to establish the value of T_o.

X4.2.1 When $K_{Jc(med)}$ is equal to or greater than 83 MPa$\sqrt{m}$, β = 18°C **(25)**. If the 1T equivalent $K_{Jc(med)}$ is below 83 MPa$\sqrt{m}$, values of β must be increased according to the following schedule:

$K_{Jc(med)}$ 1T equivalent [A] (MPa$\sqrt{m}$)	β (°C)
83 to 66	18.8
65 to 58	20.1
[A] Round off $K_{Jc(med)}$ to nearest whole number.	

X4.2.2 To estimate the uncertainty in T_o, a standard two-tail normal deviate, Z, should be taken from statistical handbook tabulations. The selection of the con-

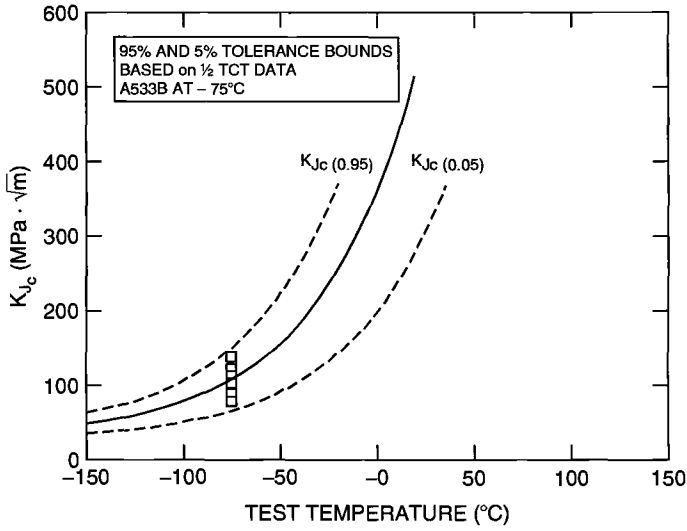

Fig. X4.1—Master Curve With Upper and Lower 95% Tolerance Bounds

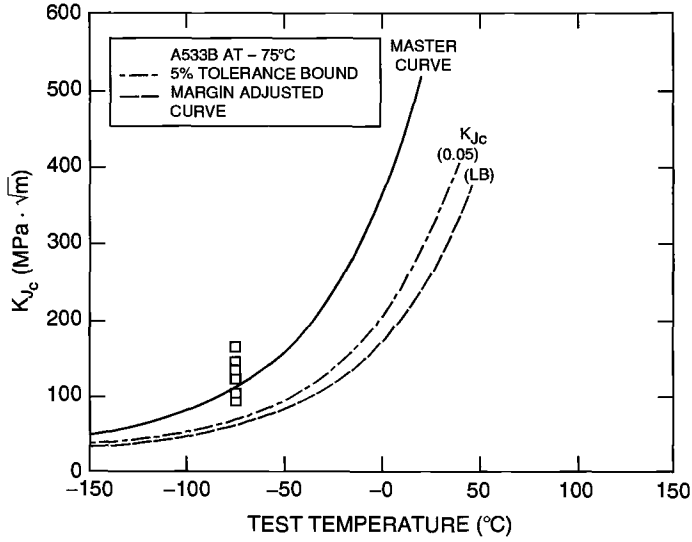

Fig. X4.2—Master Curve Showing the Difference Between 5% Tolerance Bound and Lower Bound That Includes 85% Confidence Margin on T_o

fidence limit for T_o adjustment is a matter for engineering judgment. The following example calculation is for 85% confidence (two-tail) adjustment to Eq. X4.3 for the six specimens used to determine T_o.

$$\Delta T_o = \sigma(Z_{85}) = \frac{18}{\sqrt{6}}(1.44) = 10°C \quad \text{(X4.5)}$$

$$T_o(margin) = T_o + \Delta T_o = -80° + 10° = -70°C$$

Then the margin-adjusted 5% tolerance bound of Eq. X4.3 is revised to:

$$K_{Jc(05)} = 25.2 + 36.6 \exp[0.019(T + 70)] \quad \text{(X4.6)}$$

Eq. X4.6 is plotted in Fig. X4.2 as the dashed line (L.B.).

Subject Index

Donald E. McCabe

Mr. McCabe is currently a consultant in the Metals & Ceramics Division of the Oak Ridge National Laboratory (ORNL). Although he graduated with a BS degree in Metallurgical Engineering at the University of Wisconsin, he decided to switch his interests to the new scientific discipline of fracture mechanics in 1960 and has participated in this field for 40 years. He has authored and co-authored more than 70 technical publications. He became active in ASTM committee work and has served as Secretary to the Executive Committee of E24 (now E08) for 13 years and as Chairman of the task groucation. Mr. McCabe has received the George R. Irwin Medal, the Award of Merit, the Richard L. Templin Award, and four Awards of Appreciation.

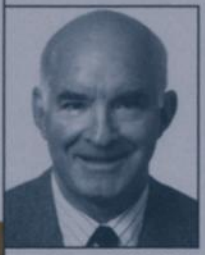

John G. Merkle

Mr. Merkle has over 40 years of experience in the fields of fracture mechanics and pressure vessel research. He worked on the Nuclear Regulatory Commission (NRC)-sponsored Heavy Section Steel Technology Program at the Oak Ridge National Laboratory (ORNL) and related projects from 1965 until his retirement in 1999. He continues to consult in the same fields at ORNL. Mr. Merkle has been a member of ASTM since 1967, serving as co-chairman of Task Group E08.08.03 while ASTM Standard E 1921 was being prepared and balloted. Mr. Merkle has a Master's degree in Civil Engineering from Cornell University, and his contributions to fracture mechanics have focused mainly on the development of physically based analytical representations of the elastic-plastic behavior of fracture toughness specimens and structural components. Mr. Merkle has received several awards from ASTM, including the George R. Irwin Medal, the Jerry L. Swedlow Lecture Award, and the ASTM Award of Merit. Mr. Merkle also participates actively in the work of Section XI of the American Society of Mechanical Engineers (ASME) Boiler and Pressure Vessel Code, pertaining to the in-service inspection and fracture mechanics evaluations for reactor pressure vessels and piping.

Dr. Kim Wallin

Dr. Kim Wallin, a research professor at VTT in Espoo, Finland, has been involved with different research topics related to experimental and theoretical fracture mechanics since 1982, and he has written more than 290 publications on the subject. Since 1993, he has held the position of research professor in fracture mechanics at VTT. He is responsible for the scientific level of the fracture mechanics research within VTT Industrial Systems. Additionally, he has had a leading role in numerous international co-operative projects dealing with advanced fracture mechanics. Dr. Wallin has been a member of ASTM International since 1991. He holds a Doctorate degree in Process and Materials Technology from the Helsinki University of Technology, where he also earned his Master of Science degree in Physical Metallurgy. Dr. Wallin's most significant scientific achievements have been connected to the theoretical modeling of brittle fracture and to the development of new engineering applications, above all in the context of the so-called "Master Curve" methodology. His research has led to a global change of the principle of brittle fracture assessment and has also given novel insight to the failure mechanisms in the case of ductile fracture.

ISBN 0-8031-3368-5
Stock #: MNL52

www.astm.org